ELSEVIER

Contents lists available at ScienceDirect

Results in Engineering

journal homepage: www.sciencedirect.com/journal/results-in-engineering



Research paper



Numerical analysis of Lucas polynomials innovative technique within the Galerkin strategy for solving fuzzy-type differential models with an application in the electrical circuit engineering field

Omar Abu Arqub ^{a,*} , Marwan Abukhaled ^b, Hind Sweis ^{c,*}, Nabil Shawagfeh ^d

- ^a Department of Mathematics, Faculty of Science, Al-Balga Applied University, Salt 19117, Jordan
- ^b Department of Mathematics and Statistics, American University of Sharjah, Sharjah 26666, United Arab Emirates
- Department of Data Science, Faculty of Data Science, Arab American University, Ramallah P600, Palestine
- ^d Department of Mathematics, Faculty of Science, The University of Jordan, Amman 11942, Jordan

ARTICLE INFO

Keywords: Fuzzy-type differential model Crisp-type differential model Lucas orthogonal polynomials Galerkin strategy Strongly generalized differentiability Series resistor-inductor circuit

MSC: 34A07 65L60 11B39

ABSTRACT

Modeling uncertain dynamical models with fuzzy differential approaches is important in different practical fields. This investigation presents an innovative technique for solving uncertain models using Lucas polynomials within the Galerkin strategy. We establish essential definitions and preliminary results of the Lucas polynomials and derive the iterative technique for numerically approximating solutions using the Galerkin strategy. The fuzzy differential models are transformed into algebraic transcendental equations, and the numerically estimated solutions are derived by solving the resultant system. To modify and adjust the technique's efficacy, we carry out and validate the convergence and error estimation requirements. The utilized numerical procedure brings five great benefits: it recognizes solutions globally, shows off high levels of accuracy and efficiency, excels in solving nonlinearity terms, is still unaffected by discretization errors and computational round-off matters, and uses a small number of iterative steps. To demonstrate the importance of fuzzy-type models, we go into great depth about an electrical engineering application and highlight the significance of its uncertainty modeling. By eliminating the importance of wide computational resources, the approach used displays superior performance compared to existing methodologies. Several comparison tables with the Hilpert kernel strategy are tabulated to test the accuracy of the Lucas Galerkin approach. The expected results have the potential to have a considerable influence on scientific and engineering sectors where uncertain and dependable mathematical modeling is critical.

1. Overview and problem issue

The ambiguous calculus and FTDMs have garnered considerable scholarly interest owing to their remarkable capacity to address intricate real-world systems characterized by vagueness and imprecision [1–3]. By integrating ambiguous sets into classical mathematical frameworks, fuzzy analysis represents a groundbreaking advancement, offering a rigorous and precise methodology for modeling systems fraught with uncertainty or incomplete data. The CTDMs are fundamental tools in modeling physical phenomena across diverse fields. Whilst CTDMs offer clarity in well-defined systems, real-world complexities often introduce uncertainty from sources like experimental data, resource errors, and initial conditions. The FTDMs provide a suitable mathematical framework to represent uncertain systems instead of CTDMs. Solving FTDMs

with specified FTICs is crucial for addressing practical problems with uncertain parameters. Analytical solutions for FTDMs are limited, especially in nonlinear and nonhomogeneous cases, in addition to the time taken to find the required solutions. Consequently, numerical analysis is essential for obtaining approximate solutions in most real-world applications modeled by FTDMs.

The FTDMs with restricted FTICs are typically handled by three main techniques. The 1st one treats the initial data and the resulting solution as fuzzy functions, requiring fuzzy derivatives, often calculated using the Hukuhara derivative [4,5]. This scheme tends to produce increasingly uncertain solutions over time, diverging from the behavior of crisp solutions. The 2nd one converts the FTDMs into a crisp differential inclusion [6,7]. A significant limitation here is the absence of a fuzzy differential operator, leading to solutions that may not be interval-valued. The 3rd one applies Zadeh's extension principle by

E-mail addresses: o.abuarqub@bau.edu.jo (O. Abu Arqub), hind.sweis@aaup.edu (H. Sweis).

https://doi.org/10.1016/j.rineng.2025.106298

^{*} Corresponding authors.

Nomenclatures

LOP-GS Lucas orthogonal polynomial - Galerkin strategy

FTDM Fuzzy-type differential model CTDM Crisp-type differential model FTIC Fuzzy-type initial condition CTIC Crisp-type initial condition

SGD Strongly generalized differentiability SRIC Series resistor-inductor circuit

HKS Hilpert kernel strategy

solving the corresponding CTDMs and then substituting fuzzy values for the constant terms, whilst the fuzzy arithmetic is subsequently used to obtain the final solution [8,9]. This scheme requires reformulating the solution in a fuzzy framework, making it less user-friendly and computationally demanding. To overcome these challenges, the concept of SGD was unveiled and offered greatly in [10]. This approach allows for two potential local solutions to FTDM and can be executed on a wider assortment of fuzzy models than other differentiation schemes [11–14]. Similar to the well-established study of CTDMs, researchers have extensively explored solving FTDMs. Various approaches, including SGD, Hukuhara differentiability, and the extension principle, have been employed in these investigations. For a comprehensive overview of these schemes, their applications, and theoretical underpinnings, readers are referred to the works of [4–15].

Besides utilizing useful insights into improving the convergence and accuracy of fuzzy solutions over a wide assortment of FTDMs by thoroughly exploring the LOP-GS and its variants, our analysis in this essay aims to expand the use of the LOP within the GS and employ SGD to obtain numerical solutions for the following FTDM:

$$\mathfrak{S}'(\xi) = \mathsf{E}(\xi, \mathfrak{S}(\xi)),\tag{1}$$

controlled within FTIC

$$\mathfrak{H}(a) = \mathscr{L}. \tag{2}$$

Herein, $a \leq \xi \leq b$, $\xi : C([a, b] \times \mathbb{R}_{\mathscr{T}} \to \mathbb{R}_{\mathscr{T}})$, $\mathfrak{H} : C([a, b] \to \mathbb{R}_{\mathscr{T}})$, $\mathscr{L} \in \mathbb{R}_{\mathscr{T}}$, and $a, b \in \mathbb{R}$, in which

$$\mathbb{R}_{\mathscr{F}} = \left\{ \begin{array}{l} \textbf{a}: \mathbb{R} \rightarrow [0,1] \mid \textbf{a} \text{ is upper semicontinuous of} \\ \text{bounded support, normal, and convex.} \end{array} \right\} \tag{3}$$

To solve (1) and (2) numerically, we use an innovative technique based on the GS, which is expanded using the LOPs that are currently tried and have a vital role in mathematics and physics. The LOPs display a recursive relationship, and through the orthogonality benefits, one can represent any function as a collection of orthogonal bases. Many researchers have adopted the LOPs, and a lot of literature detailing these numerical-based approaches, along with their different characteristics, features, and practical applications, as stated in [16–20]. The LOPs have been utilized to handle the Sobolev model [21], to solve the sinh-Gordon model [22], to approximate the electrohydrodynamics flow fractional model [23], to handle the linearization problem [24], and to approximate the generalized Burgers model [25]. A key area of LOPs involves determining connection coefficients, which establish relationships between different orthogonal polynomial sets and focus on evaluating the coefficients utilized in [26–28].

To facilitate our work and approach clearly, here's a set of the novelty, motivation, and limitations of our findings:

Novelty:

1. This work introduces the application of the LOP-GS framework for the first time in the context of solving FTDMs, offering a new class of basis functions for this purpose.

- 2. Unlike traditional polynomial bases (e.g., Legendre, Chebyshev), the LOPs exhibit specific orthogonal properties that enhance stability and accuracy, particularly in handling the imprecision inherent in fuzzy models.
- 3. The proposed technique is further validated through a practical application in electrical circuit engineering, demonstrating both the theoretical rigor and real-world relevance of the method.
- 4. A detailed convergence analysis and error estimation are provided, filling a gap in the literature regarding the theoretical underpinnings of fuzzy Galerkin-based solvers using non-classical polynomial bases.

• Motivation

- 1. Many real-world engineering systems, such as electrical circuits, are influenced by uncertainties and imprecise parameters that are best modeled using FTDMs. However, existing numerical methods often lack robustness or fail to guarantee convergence under fuzzy frameworks.
- 2. The motivation behind using LOPs arises from their recursive structure and computational advantages, which are well-suited for implementing spectral or semi-spectral methods.
- 3. The study aims to bridge the gap between analytical rigor and applicability, offering a method that is both mathematically grounded and practically implementable in engineering systems affected by uncertainty.

• Limitation

- 1. The current approach is limited to linear FTDMs; extending it to nonlinear or strongly coupled systems remains a challenge and is suggested for future research.
- 2. The implementation relies on the precise construction of the Lucas basis and assumes smoothness of the underlying fuzzy functions, which might limit its performance in cases involving discontinuities or sharp gradients.
- 3. The method has been tested on a specific class of fuzzy initial value problems in electrical engineering; broader validation across diverse domains and model types is required to generalize its effectiveness.

In the context of approximation theory, both polynomial and nonpolynomial functions have played pivotal roles in the development of efficient numerical methods [29,30]. Polynomial functions, particularly orthogonal polynomials such as Lucas, Legendre, Chebyshev, and Hermite, are widely used due to their excellent convergence properties and ease of implementation within spectral and Galerkin frameworks. They provide a powerful basis for approximating smooth solutions of differential and integral models. Likewise, non-polynomial functions, such as trigonometric, exponential, and spline-based functions, are often employed when the solution exhibits periodic behavior, discontinuities, or other features that are difficult to capture with polynomial bases alone. The choice between polynomial and non-polynomial approximating functions depends on the nature of the problem, the desired accuracy, and the computational complexity. This study focuses on a class of orthogonal polynomial bases, namely the LOPs, which offer a new perspective within the framework of FTDMs.

The following outlines our main contributions and highlights the significance of the proposed LOP-GS:

- Novel use of Lucas orthogonal polynomials: This work is among the first to integrate LOPs within the GS for solving FTDMs. Unlike commonly used polynomial bases, the LOPs offer a recursive structure with favorable computational properties, enabling efficient and accurate approximation.
- Extension to fuzzy modeling: The LOP-GS extends classical Galerkin frameworks to handle fuzzy-valued functions, which are essential for modeling systems with uncertainty and imprecision, particularly relevant in engineering applications.
- 3. Theoretical validation: A rigorous convergence analysis and error estimation are provided, proving that the LOP-GS is both

Algorithm 1 Procedures for finding solutions of FTDM (1) and (2) according to SGD.

O. Abu Arqub et al.

Situation 1.	When $\mathfrak{H}(\xi)$ i	is (1)-SGD, use $[D_1 \mathfrak{F}(\xi)]^{\zeta}$ and execute the undermentioned:		
	Process i.	Figurate the set of CTDMs: $\begin{cases} \hat{\mathfrak{S}}_{1\zeta}(\xi) = E_{1\zeta}(\xi, \hat{\mathfrak{D}}_{1\zeta}(\xi), \hat{\mathfrak{D}}_{2\zeta}(\xi)), \\ \hat{\mathfrak{D}}_{2\zeta}(\xi) = E_{2\zeta}(\xi, \hat{\mathfrak{D}}_{1\zeta}(\xi), \hat{\mathfrak{D}}_{2\zeta}(\xi)), \\ \hat{\mathfrak{D}}_{1\zeta}(a) = \mathscr{L}_{1\zeta}, \\ \hat{\mathfrak{D}}_{2\zeta}(a) = \mathscr{L}_{2\zeta}. \end{cases}$		
	Process ii. Process iii.	$\begin{split} & \text{Check that } [\mathring{\mathfrak{D}}_{1\zeta}(\xi),\mathring{\mathfrak{D}}_{2\zeta}(\xi)] \text{ and } \left[\mathring{\mathfrak{D}}_{1\zeta}'(\xi),\mathring{\mathfrak{D}}_{2\zeta}'(\xi)\right] \text{ are valid} \\ & \forall \zeta \in [0,1]. \\ & \text{Fabricate the } (1)\text{-solution } \mathring{\mathfrak{D}}(\xi) \text{ with } [\mathring{\mathfrak{D}}(\xi)]^{\zeta} = [\mathring{\mathfrak{D}}_{1\zeta}(\xi), \\ & \mathring{\mathfrak{D}}_{2\zeta}(\xi)]. \end{split}$		
Situation 2.	When $\mathfrak{H}(\xi)$ is (2)-SGD, use $[D_2\mathfrak{H}(\xi)]^{\zeta}$, and execute the undermentioned:			
	Process i.	Figurate the set of CTDMs: $\begin{cases} \hat{\mathfrak{D}}_{1\zeta}'(\xi) = \mathfrak{E}_{2\zeta}(\xi, \hat{\mathfrak{D}}_{1\zeta}(\xi), \hat{\mathfrak{D}}_{2\zeta}(\xi)), \\ \hat{\mathfrak{D}}_{2\zeta}'(\xi) = \mathfrak{E}_{1\zeta}(\xi, \hat{\mathfrak{D}}_{1\zeta}(\xi), \hat{\mathfrak{D}}_{2\zeta}(\xi)), \\ \hat{\mathfrak{D}}_{1\zeta}(a) = \mathscr{L}_{1\zeta}, \\ \hat{\mathfrak{D}}_{2\zeta}(a) = \mathscr{L}_{2\zeta}. \end{cases}$		
	Process ii. Process iii.	Check that $[\mathfrak{G}_{1\zeta}(\xi),\mathfrak{G}_{2\zeta}(\xi)]$, and $[\mathfrak{G}_{2\zeta}'(\xi),\mathfrak{G}_{1\zeta}'(\xi)]$ are valid $\forall \zeta \in [0,1]$. Fabricate the (2)-solution $\mathfrak{G}(\xi)$ with $[\mathfrak{G}(\xi)]^{\zeta} = [\mathfrak{G}_{1\zeta}(\xi),\mathfrak{G}_{2\zeta}(\xi)]$.		

Algorithm 2
Procedures for finding LOP-GS solutions of FTICs (1) and (2) in Situation 1 of Algorithm 1.

Input	Initial data: \mathcal{L} , ζ , m , N , and M ;
	LOPs concering $\delta_{1\zeta}$, $\delta_{2\zeta}$, $\delta_{1\zeta}$, $\delta_{2\zeta}$, $\delta_{1\zeta}$, and $\delta_{2\zeta}$.
Routine i.	Within $\xi \in [a,b]$ and $\zeta \in [0,1]$ fixed N and M :
	Step 1. Set $\xi_j = a + \frac{b-a}{N}j$ with $j = 0, 1, \dots, N$;
	Step 2. Set $\zeta_{\eta} = \frac{1}{M} \eta$ with $\eta = 0, 1, \dots, M$;
Routine ii.	Within $i = 0, 1, \dots, m-1$ evaluate $R_{1\zeta}(\xi)$ and $R_{2\zeta}(\xi)$.
Routine iii.	Within $i=1,2,\cdots,m-1$ evaluate
	$\left\{egin{aligned} \int_0^1 R_{1\zeta}(\xi) \phi_1(\xi) d\xi &= 0, \ \int_0^1 R_{1\zeta}(\xi) \phi_1(\xi) d\xi &= 0, \ \sum_{i=0}^{n-1} c_i \phi_i(a) &= \mathscr{L}_{1\zeta}, \ \sum_{i=0}^{n-1} d_i \phi_i(a) &= \mathscr{L}_{2\zeta}. \end{aligned} ight.$
Routine iv.	Solve the gained $2m$ transcendental equations and find c_i and d_i with i
	$=0,\cdots,$ m $-1.$
Routine v.	Substitute c_i and d_i within $i=0,\cdots, \mathbb{n}$ on LOPs of $\mathfrak{H}_{1\zeta_{\eta}\mathbb{n}}\left(\xi_j\right)$ and
	$\mathfrak{H}_{2\zeta_{\eta^{\mathrm{ll}}}}ig(\xi_{\mathrm{j}}ig).$
Output	The value of $\mathfrak{H}_{1\xi_{\eta}}\left(\xi_{j}\right)$ and $\mathfrak{H}_{2\xi_{\eta}}\left(\xi_{j}\right)$.

mathematically sound and numerically stable. This theoretical foundation is often lacking in similar work involving non-standard orthogonal bases.

- 4. Application to electrical circuit models: To demonstrate real-world significance, the proposed approach is applied to a fuzzy electrical circuit problem. The results show that the LOP-GS yields higher accuracy and faster convergence compared to existing techniques.
- Computational advantages: The Lucas basis leads to a sparse system structure in the Galerkin formulation, reducing the computational cost without sacrificing accuracy, an advantage for real-time simulations.

The LOPs and their generalizations are basic tools across fields, like physics, computer science, statistics, chemistry, and mathematics

[16–28]. Analytically, the LOP-GS is a straightforward technique to perform, freed from the necessity for complicated mathematical tools or specialized techniques in programming. Here are the main steps in the mathematical outline of the GS within LOP, whilst detailed descriptions are given in Algorithm 2.

- Step 1: Choosing the approximation: assume the required solution is a linear combination of the LOPs basis functions.
- Step 2: Formulating the residual: define a new operator by translating all terms in the FTDM into LHS.
- Step 3: Enforcing the GS condition: the GS requires that the residual be orthogonal to each LOP basis function.
- Step 4: Solving the obtained transcendental system: simplify the system, use the linearity condition, and use matrix form representation.
- Step 5: Construct the approximate solution: infer the finite summation of multiples of the LOPs basis functions with the obtained unknown coefficients from Step 4.

This essay is structured into several sections. Following the introduction, Section 2 establishes essential definitions and preliminary results for the fuzzy analysis. Section 3 provides an overview of FTDM theory and its solution algorithm. Section 4 constructs the LOP within GS to facilitate our numerical approach. Section 5 outlines the theoretical underpinnings, like convergence and error, for the truncated approximate solutions. An iterative technique for numerically approximating solutions is detailed in Section 6, along with two physical applications. The efficacy of the method is demonstrated through some findings and comparative analysis in Section 7. Finally, Section 8 concludes the paper with a summary of key findings and potential future directions.

2. Notes and specifications

The fundamental study of integrals and derivatives of uncertain functions is known as fuzzy calculus. This area of mathematics, which has been studied in great detail recently, has become a powerful and effective tool for mathematically expressing a variety of scientific and engineering phenomena. Here, we will provide several key terms from fuzzy calculus theory and preliminary research. We shall use the idea of SGD, a variation of Hukuhara differentiability that efficiently processes FTDMs while discussing the concept of a fuzzy derivative.

Let $S \neq \emptyset$, a fuzzy set $\mathbb a$ in S is an $\mathbb a: S \rightarrow [0,1]$. Thus, $\mathbb a(\kappa)$ is analyzed as the degree of membership of κ in $\mathbb a$. An $\mathbb a$ on $\mathbb R$ is convex if $\forall \kappa_1, \kappa_2 \in \mathbb R$ and $\forall \omega \in [0, 1]$, $\mathbb a(\omega \kappa_1 + (1 - \omega)\kappa_2) \geq \min\{\mathbb a(\kappa_1), \mathbb a(\kappa_2)\}$; is upper semicontinuous if $\{\kappa \in \mathbb R | \mathbb a(\kappa) \geq \zeta\}$ is closed $\forall \zeta \in [0, 1]$; and is normal if $\exists \kappa \in \mathbb R$ with $\mathbb a(\kappa) = 1$. The support of $\mathbb a$ is $\{\kappa \in \mathbb R | \mathbb a(\kappa) > 0\}$.

For all $\zeta \in (0, 1]$, put $[a]^{\zeta} = \{\kappa \in \mathbb{R} | a(\kappa) \ge \zeta\}$ and $[a]^0 = \overline{\{\kappa \in \mathbb{R} | a(\kappa) > 0\}}$. Then the following are held:

- An $a \in \mathbb{R}_{\mathscr{T}}$ iff $[a]^{\zeta}$ is a compact convex subset of \mathbb{R} within $[a]^1 \neq \phi$.
- If $a \in \mathbb{R}_{\mathcal{F}}$, then $[a]^{\zeta} = [a_1(\zeta), a_2(\zeta)]$, where $a_1(\zeta) = \min\{\kappa | \kappa \in [a]^{\zeta}\}$ and $a_2(\zeta) = \max\{\kappa | \kappa \in [a]^{\zeta}\}$.
- The symbol $[a]^{\zeta}$ is the ζ -cut formation of $a \in \mathbb{R}_{\mathscr{F}}$.

Theorem 1. [31] Presume that $a_1, a_2 : [0,1] \to \mathbb{R}$ with $a(\kappa) = \sup\{\zeta | a_1(\zeta) \le \kappa \le a_2(\zeta)\}$ meet the outlined criteria:

- 1. $a_1<\infty$ is a non-decreasing and $a_2<\infty$ is a non-increasing with $a_1(1)\leq a_2(1).$
- 2. $\forall k \in (0, 1]$, $\lim_{\zeta \to k^-} \mathbb{a}_1(\zeta) = \mathbb{a}_1(k)$ and $\lim_{\zeta \to k^-} \mathbb{a}_2(\zeta) = \mathbb{a}_2(k)$ with $\lim_{\zeta \to 0^+} \mathbb{a}_1(\zeta) = \mathbb{a}_1(0)$ and $\lim_{\zeta \to 0^+} \mathbb{a}_2(\zeta) = \mathbb{a}_2(0)$.

Then $a: \mathbb{R} \rightarrow [0,1]$ is in $\mathbb{R}_{\mathcal{F}}$ with formation $[a_1(\zeta),a_2(\zeta)]$. As well, if $a \in \mathbb{R}_{\mathcal{F}}$ with formation $[a_1(\zeta),a_2(\zeta)]$, then a_1 and a_2 are affirmed (1) and (2).

Henceforth, $\forall \zeta \in (0, 1]$, we write $a_{1\zeta}$ and $a_{2\zeta}$ instead of $a_1(\zeta)$ and $a_2(\zeta)$, simultaneously.

Definition 1. [32] In $\mathbb{R}_{\mathscr{T}}$ within $a, b \in \mathbb{R}_{\mathscr{T}}$, we use

$$\begin{cases} D: \mathbb{R}_{\mathscr{T}} \times \mathbb{R}_{\mathscr{T}} \rightarrow \mathbb{R}^+ \cup \{0\}, \\ D(\mathbf{a}, \mathbf{b}) = \sup_{0 \leq \zeta \leq 1} \max\{|\mathbf{a}_{1\zeta} - \mathbf{b}_{1\zeta}|, |\mathbf{a}_{2\zeta} - \mathbf{b}_{2\zeta}|\}. \end{cases}$$
 (4)

If $a, b \in \mathbb{R}_{\mathscr{T}}$, then $\forall \zeta \in [0, 1]$, one has

$$[a + b]^{\zeta} = [a]^{\zeta} + [b]^{\zeta} = [a_{1\zeta} + b_{1\zeta}, a_{2\zeta} + b_{2\zeta}],$$

$$[wa]^{\zeta} = w[a]^{\zeta} = [\min\{wa_{1\zeta}, wa_{2\zeta}\}, \max\{wa_{1\zeta}, wa_{2\zeta}\}],$$

$$\begin{aligned} [\mathtt{a}\mathtt{b}]^\zeta = [\mathtt{a}]^\zeta [\mathtt{b}]^\zeta = [& \min \{ \mathtt{a}_{1\zeta} \mathtt{b}_{1\zeta}, \mathtt{a}_{1\zeta} \mathtt{b}_{2\zeta}, \mathtt{a}_{2\zeta} \mathtt{b}_{1\zeta}, \mathtt{a}_{2\zeta} \mathtt{b}_{2\zeta} \}, \\ & \max \{ \mathtt{a}_{1\zeta} \mathtt{b}_{1\zeta}, \mathtt{a}_{1\zeta} \mathtt{b}_{2\zeta}, \mathtt{a}_{2\zeta} \mathtt{b}_{1\zeta}, \mathtt{a}_{2\zeta} \mathtt{b}_{2\zeta} \}]. \end{aligned}$$

$$a = b$$
 iff $[a]^{\zeta} = [b]^{\zeta}$ iff $a_{1\zeta} = b_{1\zeta}$ and $a_{2\zeta} = b_{2\zeta}$. (5)

Let $\mathbb{a}, \mathbb{b} \in \mathbb{R}_{\mathscr{T}}$, if $\exists \mathbb{c} \in \mathbb{R}_{\mathscr{T}}$ with $\mathbb{a} = \mathbb{b} + \mathbb{c}$ or $\mathbb{c} = \mathbb{a} \ominus \mathbb{b}$, then \mathbb{c} is a Hukuhara difference. Here, the outlined criteria are met:

- $a \ominus b \neq a + (-1)b = a b$.
- If $a \ominus b$ exists, then $[a \ominus b]^{\zeta} = [a_{1\zeta} b_{1\zeta}, a_{2\zeta} b_{2\zeta}]$.

Definition 2. [33] Let $\mathfrak{H}: [a,b] \to \mathbb{R}_{\mathscr{F}}$ and $\xi_0 \in [a,b]$. An $\mathfrak{H}: \mathbb{H}: \mathbb$

1. $\forall \lambda > 0$ properly close to 0, $\mathfrak{H}(\xi_0 + \lambda) \ominus \mathfrak{H}(\xi_0)$, $\mathfrak{H}(\xi_0) \ominus \mathfrak{H}(\xi_0 - \lambda)$ exist

$$\lim_{\lambda \to 0^+} \frac{\mathfrak{D}(\xi_0 + \lambda) \ominus \mathfrak{D}(\xi_0)}{\lambda} = \lim_{\lambda \to 0^+} \frac{\mathfrak{D}(\xi_0) \ominus \mathfrak{D}(\xi_0 - \lambda)}{\lambda} = \mathfrak{D}'(\xi_0). \tag{6}$$

2. $\forall \lambda > 0$ properly close to 0, $\mathfrak{F}(\xi_0) \ominus \mathfrak{F}(\xi_0 + \lambda)$, $\mathfrak{F}(\xi_0 - \lambda) \ominus \mathfrak{F}(\xi_0)$ exist with

$$\lim_{\lambda \to 0^{+}} \frac{\mathfrak{G}(\xi_{0}) \ominus \mathfrak{G}(\xi_{0} + \lambda)}{-\lambda} = \lim_{\lambda \to 0^{+}} \frac{\mathfrak{G}(\xi_{0} - \lambda) \ominus \mathfrak{G}(\xi_{0})}{-\lambda} = \mathfrak{G}'(\xi_{0}). \tag{7}$$

Remark 1. The limit is taken in $(\mathbb{R}_{\mathcal{T}}, D)$, and at $\{a, b\}$, we examine one-sided derivatives. If \mathfrak{F} is differentiable $\forall \xi \in [a, b]$, then \mathfrak{F} is differentiable on [a, b]. In Definition 2, the 1st type aligns with the Hukuhara derivative utilized in [34].

Definition 3. [35] Let $\mathfrak{G}: [a,b] \to \mathbb{R}_{\mathscr{T}}$. An \mathfrak{G} is (1)-SGD on [a,b] if it is differentiable in type (1) of Definition 2 with derivative $D_1\mathfrak{G}$. Similarly, an \mathfrak{G} is (2)-SGD on [a,b] if it is differentiable in type (2) of Definition 2 with derivative $D_2\mathfrak{G}$.

Theorem 2. [35] Let $\mathfrak{H}: [a,b] \to \mathbb{R}_{\mathscr{F}}$ and $[\mathfrak{H}(\xi)]^{\zeta} = [\mathfrak{H}_{1\zeta}(\xi), \mathfrak{H}_{2\zeta}(\xi)]$. Then $\forall \zeta \in [0,1]$, one has

- 1. If \mathfrak{F} is (1)-SGD on [a,b], then $\mathfrak{F}_{1\zeta}$ and $\mathfrak{F}_{2\zeta}$ are differentiable on [a,b] with $[D_1\mathfrak{F}(\xi)]^{\zeta} = [\mathfrak{F}_{1\zeta}^{'}(\xi),\mathfrak{F}_{2\zeta}^{'}(\xi)]$.
- 2. If \mathfrak{F} is (2)-SGD on [a,b], then $\mathfrak{F}_{1\zeta}$ and $\mathfrak{F}_{2\zeta}$ are differentiable on [a,b] with $[D_2\mathfrak{F}(\xi)]^{\zeta} = [\mathfrak{F}_{2\zeta}^{'}(\xi),\mathfrak{F}_{1\zeta}^{'}(\xi)]$.

3. Necessities and algorithm of the FTDM

While physical systems often exhibit deterministic behavior, uncertainties can arise from measurement processes, particularly when determining initial conditions. To account for such uncertainties, fuzzy numbers can be employed to represent initial parameters. This necessitates the exploration of perspectives involving FTDMs and FTICs. In essence, when a system's starting point is inherently fuzzy, the subsequent solution trajectory also becomes fuzzy, demanding the concept of a fuzzy derivative.

Problem formulation is typically the most crucial aspect of the procedure, encompassing the determination of the ζ -cut formation for the nonlinear term, the choice of SGD type, and the partitioning of FTICs. Subsequently, FTDM is initially expressed as a standard set of CTDMs, followed by the discretized version of FTDM. To enable the application of the LOP-GS, the fuzzy function is expressed in the ζ -cut formation as $[\mathfrak{F}(\xi)]^{\zeta} = [\mathfrak{F}_{1\zeta}(\xi), \mathfrak{F}_{2\zeta}(\xi)]$, and $[\mathfrak{F}(a)]^{\zeta} = [\mathscr{L}_{1\zeta}, \mathscr{L}_{2\zeta}]$. Through the consideration of the ζ -cut formation on both sides of (1) and (2), one can articulate

$$[\mathfrak{F}'(\xi)]^{\zeta} = [\mathfrak{E}(\xi, \mathfrak{F}(\xi))]^{\zeta},\tag{8}$$

controlled within CTDMs set

$$[\mathfrak{H}(a)]^{\zeta} = [\mathscr{L}]^{\zeta},\tag{9}$$

where the set gives the endpoints of $[\mathcal{E}(\xi, \mathfrak{H}(\xi))]^{\zeta}$ is

$$\begin{split} & \left[\boldsymbol{\xi}(\boldsymbol{\xi}, \boldsymbol{\mathfrak{G}}(\boldsymbol{\xi})) \right]^{\boldsymbol{\zeta}} = \left[\boldsymbol{\xi}_{1\boldsymbol{\zeta}}(\boldsymbol{\xi}, \boldsymbol{\mathfrak{G}}(\boldsymbol{\xi})), \boldsymbol{\xi}_{2\boldsymbol{\zeta}}(\boldsymbol{\xi}, \boldsymbol{\mathfrak{G}}(\boldsymbol{\xi})) \right] \\ & = \left[\boldsymbol{\xi}_{1\boldsymbol{\zeta}}(\boldsymbol{\xi}, \boldsymbol{\mathfrak{G}}_{1\boldsymbol{\zeta}}(\boldsymbol{\xi}), \boldsymbol{\mathfrak{G}}_{2\boldsymbol{\zeta}}(\boldsymbol{\xi})), \boldsymbol{\xi}_{2\boldsymbol{\zeta}}(\boldsymbol{\xi}, \boldsymbol{\mathfrak{G}}_{1\boldsymbol{r}}(\boldsymbol{\xi}), \boldsymbol{\mathfrak{G}}_{2\boldsymbol{\zeta}}(\boldsymbol{\xi})) \right]. \end{split} \tag{10}$$

The formulation presented in (8–10), along with the identification of Theorems 1 and 2, elucidates the approach to handling numerical solutions of FTDMs. It is possible to transform the original FTDM into a set of CTDMs. Consequently, the numerical methods can be directly applied to the resultant CTDM system.

Definition 4. [35] Let $\mathfrak{F}: [a,b] \to \mathbb{R}_{\mathscr{F}}$ such that $D_1\mathfrak{F}$ or $D_2\mathfrak{F}$ exists. If \mathfrak{F} and $D_1\mathfrak{F}$ satisfy FTDM (1) and (2), \mathfrak{F} is called a (1)-solution. Similarly, if \mathfrak{F} and $D_2\mathfrak{F}$ satisfy FTDM (1) and (2), \mathfrak{F} is called a (2)-solution.

An $\mathcal{E}: [a,b] \times \mathbb{R}_{\mathcal{F}} \to \mathbb{R}_{\mathcal{F}}$ is continuous at (ξ_0, z_0) in $[a,b] \times \mathbb{R}_{\mathcal{F}}$, if $\forall \varepsilon > 0$, $\exists \delta(\varepsilon, \zeta) > 0$ as $D(\mathcal{E}(\xi, z), \mathcal{E}(\xi_0, z_0)) < \varepsilon$ whenever $|\xi - \xi_0| < \delta$ and $D(z, z_0) < \delta$ at $\forall \xi \in [a,b]$ and $z \in \mathbb{R}_{\mathcal{F}}$.

Theorem 3. [35] Let $\mathcal{E} \in C([a,b] \times \mathbb{R}_{\mathcal{F}} \to \mathbb{R}_{\mathcal{F}})$ and assume $\exists k > 0$ with $D(\mathcal{E}(\xi, \mathcal{D}(\xi)), \mathcal{E}(\xi, \mathcal{D}(\xi))) \leq kD(\mathcal{D}(\xi), \mathcal{D}(\xi))$ for $\forall \xi \in [a,b]$ and $\mathcal{D}(\xi), \mathcal{D}(\xi) \in \mathbb{R}_{\mathcal{F}}$. Then, FTDM (1) and (2) have two unique solutions on [a,b]. Namely, (1)-SGD and (2)-SGD.

Algorithm 1 aims to develop a method for solving (1) and (2) using their ζ -cut formations. The resulting set will consist of two CTDM systems for each SGD type.

Situation 2 in Algorithm 1 is an extension of the procedure used in [36], where the derivative is considered in the 2nd form of Definition 3. So, in Situation 2, a new solution for (1) and (2) is obtained.

An $g:[a,b]\times\mathbb{R}^2\to\mathbb{R}$ is equicontinuous on [a,b] if $\forall \varepsilon>0$ and $\forall (\xi,\mathfrak{H},\mathscr{H}), (\xi,\mathfrak{H},$

Theorem 4. [37] Given FTDM (1) and (2) and $\mathcal{E}: [a,b] \times \mathbb{R}_{\mathcal{T}} \to \mathbb{R}_{\mathcal{T}}$ with

1.
$$[\mathsf{E}(\xi,\mathfrak{H}(\xi))]^{\zeta} = [\mathsf{E}_{1\zeta}(\xi,\mathfrak{H}_{1\zeta}(\xi),\mathfrak{H}_{2\zeta}(\xi)), \mathsf{E}_{2\zeta}(\xi,\mathfrak{H}_{1\zeta}(\xi),\mathfrak{H}_{2\zeta}(\xi))].$$

- 2. $\xi_{1\zeta}$ and $\xi_{2\zeta}$ are equicontinuous functions on [a,b].
- 3. $\exists L > 0$ as $\forall \zeta \in [0,1]$, we have

$$\begin{cases} |\mathsf{E}_{\mathsf{1}\zeta}(\xi, \mathfrak{G}_{\mathsf{1}}(\xi), \wp_{\mathsf{1}}(\xi)) - \mathsf{E}_{\mathsf{1}\zeta}(\xi, \mathfrak{G}_{\mathsf{2}}(\xi), \wp_{\mathsf{2}}(\xi))| \leq L \max\{|\mathfrak{G}_{\mathsf{1}}(\xi) - \mathfrak{G}_{\mathsf{2}}(\xi)|, |\wp_{\mathsf{1}}(\xi) - \wp_{\mathsf{2}}(\xi)|\}, \\ |\mathsf{E}_{\mathsf{2}\zeta}(\xi, \mathfrak{G}_{\mathsf{1}}(\xi), \wp_{\mathsf{1}}(\xi)) - \mathsf{E}_{\mathsf{2}\zeta}(\xi, \mathfrak{G}_{\mathsf{2}}(\xi), \wp_{\mathsf{2}}(\xi))| \leq L \max\{|\mathfrak{G}_{\mathsf{1}}(\xi) - \mathfrak{G}_{\mathsf{2}}(\xi)|, |\wp_{\mathsf{1}}(\xi) - \wp_{\mathsf{2}}(\xi)|\}. \end{cases}$$

$$\tag{11}$$

Then, for (1)-SGD, FTDM (1) and (2), and the set of CTDM in Process I - Situation 1 are equivalent, and for (2)-SGD, FTDM (1) and (2), and the set of CTDM in Process ii - Situation 2 are equivalent.

To sum up our strategy during the evolution process for solving (1) and (2) in (1)-SGD is based on solving the set of CTDMs in Process i - Situation 1 by converting the needed functions into the corresponding LOPs and then using the GS, the problem can be converted to a group of transcendental equations that can be solved utilizing MATHEMATICA package to get the solution. Also, for (2)-SGD, we use CTDMs in Process ii - Situation 2.

4. Assemble the LOPs approximation

To facilitate descriptions, we employ GS as an innovative numerical approach. The GS is a weighted residual-based algorithm, where the weighted functions are a finite set of orthogonal bases. Afterward, we construct the LOP-GS using the LOPs as the weighting functions. Undoubtedly, theorems of convergence and error are utilized too.

To minimize the length of this essay and avoid repetition, we will review only the first case concerning the (1)-SGD. Since the remaining case is similar, we will proceed as follows:

- First, the LOPs representing a special function over a given interval are described.
- Then, we use this representation to express the base functions in the CTDMs in Process i - Situation 1 for the (1)-SGD type in terms of LOPs.
- Next, we define the residual function needed for the GS.
- Finally, via the orthogonality between the residual and the LOPs, we transform the systems of CTDMs into algebraic sets of transcendental equations. By solving the resulting sets, we find the approximate nodal model.

Definition 5. [21] For the LOP of degree \Bbbk , the terms $\phi_{\Bbbk}(\xi)$ can be built recurrently as

$$\phi_{\Bbbk}(\xi) = \xi \phi_{\Bbbk - 1}(\xi) + \phi_{\Bbbk - 2}(\xi), \phi_{0}(\xi) = 2, \ \phi_{1}(\xi) = \xi, \ \Bbbk \geq 2. \tag{12}$$

Definition 6. [21] The LOP possesses the power from representation as

$$\phi_{\mathbb{k}}(\xi) = \mathbb{k} \sum_{r=0}^{\left\lfloor \frac{\mathbb{k}}{2} \right\rfloor} \frac{(\mathbb{k} - \mathbb{r} - 1)!}{\mathbb{r}!(\mathbb{k} - 2\mathbb{r})!} \xi^{\mathbb{k} - 2\mathbb{r}}, \mathbb{k} \ge 1.$$

$$(13)$$

To simplify, a few needed results and characteristics of the LOPs are discussed next. Here are the first few undermentioned LOPs:

$$\begin{cases} \phi_0(\xi) = 2, \\ \phi_1(\xi) = \xi, \\ \phi_2(\xi) = \xi^2 + 2, \\ \phi_3(\xi) = \xi^3 + 3\xi, \\ \phi_4(\xi) = \xi^4 + 4\xi^2 + 2. \end{cases}$$
(14)

One important relationship of LOPs is their formulas through the power form (13) within the representation

$$\phi_{\Bbbk}(\xi) = \frac{1}{\Bbbk + 1} \phi'_{\Bbbk + 1}(\xi) + \frac{1}{\Bbbk - 1} \phi'_{\Bbbk - 1}(\xi), \& \ge 2. \tag{15}$$

To facilitate, one can generate a matrix approach to the LOPs. Anyhow, let us denote the matrix with the following entries by L:

$$l_{ij} \neq 0, \forall i, l_{ij} = 0, \ j > i.$$

$$(16)$$

Clearly, L is an infinite, lower-triangular, nonsingular matrix. For example, for $\Bbbk = 6$, one find

$$L = \begin{bmatrix} 2 & 0 & 0 & \cdots & \cdots & \cdots & 0 \\ 0 & 1 & \ddots & \cdots & \cdots & \cdots & \vdots \\ 2 & 0 & 1 & \ddots & \cdots & \cdots & \vdots \\ 0 & 3 & 0 & 1 & \ddots & \cdots & \vdots \\ 2 & 0 & 4 & 0 & 1 & \ddots & \vdots \\ 0 & 5 & 0 & 5 & 0 & 1 & 0 \\ 2 & 0 & 9 & 0 & 6 & 0 & 1 \end{bmatrix}.$$

$$(17)$$

The original sequence of Lucas numbers can be extracted from the sums of the inputs in the rows of L, that is, $\sum_{r=0}^k l_{kr} = \phi_k$. Furthermore, the inputs of the columns of L correspond to the column sequences of (2, 1)-Pascal triangle, excluding the inputs l_{00} starting from 2.

To improve efficiency, if $\phi^{\xi} = [\phi_0(\xi), \phi_1(\xi), \cdots, \phi_{\Bbbk}(\xi), \cdots]^T$ and $X = \begin{bmatrix} 1, \xi, \xi^2, \cdots, \xi^{\Bbbk}, \cdots \end{bmatrix}^T$, one gains the LOPs matrix form sequence as

$$\phi^{\xi} = LX. \tag{18}$$

Generally, the power form representations and their associated inversion formula of the LOPs are essential for deriving numerous significant related relations. Anyhow, the inversion formula of (13) can be written as (for the derivation, see [26]).

$$\xi^{\mathfrak{r}} = \mathfrak{r}! \sum_{\substack{k=0 \ (k+\tau) \text{ even}}}^{\mathfrak{r}} \frac{\left(-1\right)^{\frac{\mathfrak{r}-k}{2}} \rho_{\mathbb{k}}}{\left(\frac{\mathfrak{r}-k}{2}\right)! \left(\frac{\mathfrak{r}+k}{2}\right)!} \phi_{\mathbb{k}}(\xi). \tag{19}$$

$$\rho_{\Bbbk} = \begin{cases} \frac{1}{2}, & \Bbbk = 0, \\ 1, & \Bbbk > 0. \end{cases}$$
 (20)

The orthogonality condition of LOPs derived from

$$\int_{-2}^{2} \phi_{\Bbbk}(\xi) \phi_{j}(\xi) \frac{1}{\sqrt{4 - \xi^{2}}} d\xi = \left\langle \phi_{\Bbbk}(\xi), \phi_{j}(\xi) \right\rangle = \begin{cases} 0, & \Bbbk \neq j, \\ 4\pi, & \Bbbk = j > 0, \\ 2\pi, & \Bbbk = j = 0. \end{cases}$$
 (21)

This reveals that $\forall p \in C([0,1] {
ightarrow} \mathbb{R})$ can be portrayed regarding LOPs as

$$p(\xi) \approx p_{\scriptscriptstyle m}(\xi) = \sum_{i=0}^{\scriptscriptstyle m} c_i \phi_i(\xi), \tag{22}$$

wherein $c_{i} = \langle p(\xi), \phi_{i}(\xi) \rangle$ and $\phi_{i}(\xi)$ within $i = 0, 1, \dots, n$ are the LOPs.

After presenting the abovementioned results on LOPs, we proceed to the problem formulation. Anyhow, to find an approximate solution of the CTDMs set in Situation 1, we interpolate LOPs for $\mathfrak{F}_{1r}(\xi)$ and $\mathfrak{F}_{2r}(\xi)$ as

$$\begin{cases} \tilde{\mathfrak{D}}_{1\zeta}(\xi) \approx \tilde{\mathfrak{D}}_{1\zeta^{\mathrm{m}}}(\xi) &= \sum_{\mathrm{i}=0}^{\mathrm{m}-1} c_{\mathrm{i}} \phi_{1\zeta^{\mathrm{i}}}(\xi), \\ \tilde{\mathfrak{D}}_{2\zeta}(\xi) \approx \tilde{\mathfrak{D}}_{2\zeta^{\mathrm{m}}}(\xi) &= \sum_{\mathrm{i}=0}^{\mathrm{m}-1} d_{\mathrm{i}} \phi_{2\zeta^{\mathrm{i}}}(\xi), \end{cases}$$

$$(23)$$

wherein c_i and d_i within $i=0,1,\cdots,n$ are unknown coefficients, and $\phi_{1\zeta i}(\xi)$ and $\phi_{2\zeta i}(\xi)$ are the LOPs.

Moreover, the terms approximations of $\mathfrak{G}'_{1\zeta}$, $\mathfrak{G}'_{2\zeta}$, $\mathfrak{E}_{1\zeta}$, and $\mathfrak{E}_{2\zeta}$, simultaneously, are

$$\begin{cases} \hat{\mathfrak{G}}_{1\zeta}'(\xi) \approx \hat{\mathfrak{G}}_{1\zeta_{\mathrm{B}}}'(\xi) = \sum_{\mathrm{i}=0}^{\mathrm{n}-1} c_{\mathrm{i}} \phi_{1\zeta_{\mathrm{I}}}'(\xi), \\ \\ \hat{\mathfrak{G}}_{2\zeta}'(\xi) \approx \hat{\mathfrak{G}}_{2\zeta_{\mathrm{B}}}'(\xi) = \sum_{\mathrm{i}=0}^{\mathrm{n}-1} d_{\mathrm{i}} \phi_{2\zeta_{\mathrm{I}}}'(\xi). \end{cases}$$

$$(24)$$

functions, then we integrate the multiple of the LOPs by the residuals and equate the result with zero since $R_{1\zeta}(\xi)$ and $R_{2\zeta}(\xi)$ are orthogonal with $(2\mathbb{m}-2)$ functions $\phi_0(\xi), \phi_1(\xi), \cdots, \phi_{\mathbb{m}-1}(\xi)$, thus we can get the needed $(2\mathbb{m}-2)$ algebraic equations controlled by the CTICs in Process i - Situation 1. So

$$\begin{cases} \int\limits_0^1 R_{1\zeta}(\xi)\phi_i(\xi)d\xi = 0, \ \mathbb{i} = 0, 1, \cdots, \mathbb{m} - 1, \\ \int\limits_0^1 R_{1\zeta}(\xi)\phi_i(\xi)d\xi = 0, \ \mathbb{i} = 0, 1, \cdots, \mathbb{m} - 1, \\ \sum_{i=0}^{m-1} c_i\phi_i(a) = \mathscr{L}_{1\zeta}, \\ \sum_{i=0}^{m-1} d_i\phi_i(a) = \mathscr{L}_{2\zeta}. \end{cases}$$

$$(28)$$

Hereabouts, we get an algebraic set of 2^n transcendental equations with 2^n unknown $c_0, c_1, \cdots, c_{n-1}$ and $d_0, d_1, \cdots, d_{n-1}$. Afterward, substitute the estimated constants $c_0, c_1, \cdots, c_{n-1}$ and $d_0, d_1, \cdots, d_{n-1}$ in (23) to gain the needed approximation of Situation i concerning (1)-SGD.

5. Analysis of convergence and error

To show the efficiency and adaptability of the LOP-GS approximation, this part presents and proves the convergence and captures the error estimate, ensuring that Process i - Situation 1 concerns (1)-SGD.

In the field of approximation, convergence and error are essential for

$$\begin{cases} \mathsf{E}_{1\zeta}(\xi, \mathfrak{G}_{1\zeta}(\xi), \mathfrak{G}_{2\zeta}(\xi)) \approx \mathsf{E}_{1\zeta_{\mathrm{B}}}(\xi, \mathfrak{G}_{1\zeta_{\mathrm{B}}}(\xi), \mathfrak{G}_{2\zeta_{\mathrm{B}}}(\xi)) = \mathsf{E}_{1\zeta_{\mathrm{B}}}\left(\xi, \sum_{i=0}^{\mathsf{n}-1} c_{i}\phi_{1\zeta_{i}}(\xi), \sum_{i=0}^{\mathsf{n}-1} d_{i}\phi_{2\zeta_{i}}(\xi)\right), \\ \mathsf{E}_{2\zeta}(\xi, \mathfrak{G}_{1\zeta_{\mathrm{C}}}(\xi), \mathfrak{G}_{2\zeta_{\mathrm{C}}}(\xi)) \approx \mathsf{E}_{2\zeta_{\mathrm{B}}}(\xi, \mathfrak{G}_{1\zeta_{\mathrm{B}}}(\xi), \mathfrak{G}_{2\zeta_{\mathrm{B}}}(\xi)) = \mathsf{E}_{2\zeta_{\mathrm{B}}}\left(\xi, \sum_{i=0}^{\mathsf{n}-1} c_{i}\phi_{1\zeta_{i}}(\xi), \sum_{i=0}^{\mathsf{n}-1} d_{i}\phi_{2\zeta_{i}}(\xi)\right). \end{cases}$$

Substituting (24) and (25) into Process i - Situation 1, we have

$$\begin{cases} \sum_{i=0}^{n} c_{i} \phi_{1\zeta_{i}^{i}}'(\xi) = \mathcal{E}_{1\zeta_{n}} \left(\xi, \sum_{i=0}^{n-1} c_{i} \phi_{1\zeta_{i}^{i}}(\xi), \sum_{i=0}^{n-1} d_{i} \phi_{2\zeta_{i}^{i}}(\xi) \right), \\ \sum_{i=0}^{n} d_{i} \phi_{2\zeta_{i}^{i}}'(\xi) = \mathcal{E}_{2\zeta_{n}} \left(\xi, \sum_{i=0}^{n-1} c_{i} \phi_{1\zeta_{i}^{i}}(\xi), \sum_{i=0}^{n-1} d_{i} \phi_{2\zeta_{i}^{i}}(\xi) \right). \end{cases}$$
(26)

To proceed, we use (26) to compute the needed two residuals $R_{1\zeta}(\xi)$ and $R_{2\zeta}(\xi)$ as

$$\begin{cases} R_{1\zeta}(\xi) = \sum_{i=0}^{n-1} c_{i} \phi'_{1\zeta_{i}}(\xi) - \mathcal{E}_{1\zeta_{n}} \left(\xi, \sum_{i=0}^{n-1} c_{i} \phi_{1\zeta_{i}}(\xi), \sum_{i=0}^{n-1} d_{i} \phi_{2\zeta_{i}}(\xi) \right), \\ R_{2\zeta}(\xi) = \sum_{i=0}^{n-1} d_{i} \phi'_{2\zeta_{i}}(\xi) - \mathcal{E}_{2\zeta_{n}} \left(\xi, \sum_{i=0}^{n-1} c_{i} \phi_{1\zeta_{i}}(\xi), \sum_{i=0}^{n-1} d_{i} \phi_{2\zeta_{i}}(\xi) \right). \end{cases}$$
(27)

However, when $R_{1\zeta}(\xi)=0$ and $R_{2\zeta}(\xi)=0$, one has the exact solution that handles the set of CTDMs in Situation 1. In the proposed LOP-GS approximation, we aim to minimize the residuals by making it orthogonal to the chosen LOPs, which are the basis functions used to find $\mathfrak{H}_{1\zeta}(\xi)$ and $\mathfrak{H}_{2\zeta}(\xi)$ approximations.

To find c_0, c_1, \dots, c_{n-1} and d_0, d_1, \dots, d_{n-1} , we select LOPs as weight

ensuring the accuracy and efficiency of numerical schemes, preventing divergence, and optimizing computational performance. This can symmetrize as

- Ensures numerical solutions approximate the true solution correctly.
- Prevents solutions from diverging or becoming unreliable.
- Helps select methods that converge faster with minimal computation.
- · Identifies and minimizes sources of numerical error.
- Confirms the reliability of mathematical models and simulations.

Recalling that $\mathfrak{F}_{1\zeta_{\Pi}}(\xi) = \sum_{i=0}^{n-1} c_i \phi_{1\zeta_i}(\xi)$, $\mathfrak{F}_{2\zeta_{\Pi}}(\xi) = \sum_{i=0}^{n-1} d_i \phi_{2\zeta_i}(\xi)$, $\mathfrak{F}_{\zeta_{\Pi}}(\xi) = (\mathfrak{F}_{1\zeta_{\Pi}}(\xi), \ \mathfrak{F}_{2\zeta_{\Pi}}(\xi))$, and $\mathfrak{F}_{\zeta}(\xi) = (\mathfrak{F}_{1\zeta_{L}}(\xi), \ \mathfrak{F}_{2\zeta_{L}}(\xi))$. Also, throughout the next results $\mathfrak{F}_{1\zeta_{\Pi}}(\xi) = \sum_{i=0}^{m} c_i \phi_{1\zeta_i}(\xi)$, $\mathfrak{F}_{2\zeta_{\Pi}}(\xi) = \sum_{i=0}^{m} d_i \phi_{2\zeta_i}(\xi)$, $\mathfrak{F}_{\zeta_{\Pi}}(\xi) = (\mathfrak{F}_{1\zeta_{\Pi}}(\xi), \mathfrak{F}_{2\zeta_{\Pi}}(\xi))$, and $z_{\zeta}(\xi) = (z_{1\zeta_{L}}(\xi), z_{2\zeta_{L}}(\xi))$ with $z_{1\zeta_{L}}(z_{2\zeta_{L}}(\xi)) \in L^{2}([0,1])$.

 $\begin{array}{lll} \textbf{Theorem 5.} & \textit{Presume } \left(\, \sum_{i=0}^{\infty} c_i \phi_{1\zeta_i}(\xi), \, \sum_{i=0}^{\infty} \, d_i \phi_{2\zeta_i}(\xi) \right) \textit{ be the Lucas interpolation } & \textit{of } \left(\, \mathfrak{F}_{1\zeta}(\xi), \, \mathfrak{F}_{2\zeta}(\xi) \right) & \textit{with } \quad \, \mathfrak{F}_{1\zeta}, \, \mathfrak{F}_{2\zeta} \in L^2[0,1]. \end{array}$

Proof. Let $(\mathfrak{H}_{1\zeta\mathfrak{m}}(\xi),\mathfrak{H}_{2\zeta\mathfrak{m}}(\xi))$ be any partial sum of $(\sum_{i=0}^{\infty}c_{i}\phi_{i}(\xi),\sum_{i=0}^{\infty}d_{i}\phi_{2\zeta i}(\xi))$. Then for $\mathfrak{m}>\mathfrak{m}$, one has

O. Abu Arqub et al. Results in Engineering 27 (2025) 106298

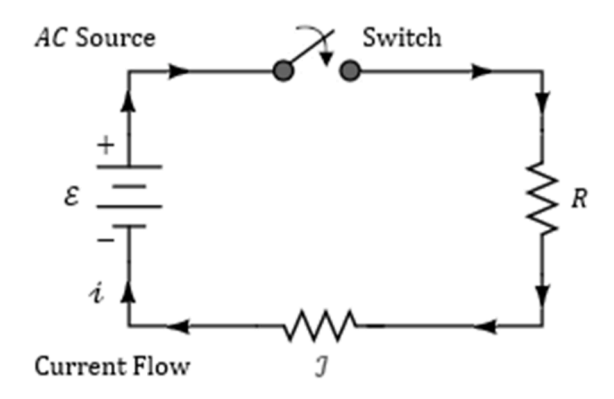


Fig. 1. Portrayal of the SRIC in its crisp version.

$$\| \tilde{\mathfrak{D}}_{\zeta_{n}}(\xi) - \tilde{\mathfrak{D}}_{\zeta_{m}}(\xi) \|^{2} = \| \begin{bmatrix} \tilde{\mathfrak{D}}_{1\zeta_{n}}(\xi) \\ \tilde{\mathfrak{D}}_{2\zeta_{n}}(\xi) \end{bmatrix} - \begin{bmatrix} \tilde{\mathfrak{D}}_{1\zeta_{m}}(\xi) \\ \tilde{\mathfrak{D}}_{2\zeta_{m}}(\xi) \end{bmatrix} \|^{2}$$

$$= \| \begin{bmatrix} \sum_{i=m+1}^{n} c_{i}\phi_{1\zeta_{i}}(\xi) \\ \sum_{i=m+1}^{n} d_{i}\phi_{2\zeta_{i}}(\xi) \end{bmatrix} \|^{2}$$

$$< \begin{bmatrix} \sum_{i=m+1}^{n} |c_{i}|^{2} \left(\frac{\pi}{2}\right) \\ \sum_{i=m+1}^{n} |d_{i}|^{2} \left(\frac{\pi}{2}\right) \end{bmatrix} .$$

$$(29)$$

By Bessel's inequality; $\sum_{i=m+1}^{n}|c_i|^2 \leq \sum_{i=m+1}^{\infty}|c_i|^2 \leq \|\mathfrak{H}_{1\zeta}\|^2 < \infty$ and $\sum_{i=m+1}^{n}|d_i|^2 \leq \sum_{i=m+1}^{\infty}|d_i|^2 \leq \|\mathfrak{H}_{2\zeta}\|^2 < \infty$. So, $\|\mathfrak{H}_{\zeta_m}(\xi) - \mathfrak{H}_{\zeta_m}(\xi)\|^2 \to 0$ as $m, m \to \infty$. Thus, $\mathfrak{H}_{\zeta_m}(\xi)$ is a Cauchy sequence and converges. Anyhow

$$\begin{cases} \hat{\mathfrak{G}}_{1\zeta_{\mathbb{R}}}^{'}(\xi) = \mathbf{E}_{1\zeta_{\mathbb{R}}}(\xi, \hat{\mathfrak{G}}_{1\zeta_{\mathbb{R}}}(\xi), \hat{\mathfrak{G}}_{2\zeta_{\mathbb{R}}}(\xi)), \\ \hat{\mathfrak{G}}_{2\zeta_{\mathbb{R}}}^{'}(\xi) = \mathbf{E}_{2\zeta_{\mathbb{R}}}(\xi, \hat{\mathfrak{G}}_{1\zeta_{\mathbb{R}}}(\xi), \hat{\mathfrak{G}}_{2\zeta_{\mathbb{R}}}(\xi)), \\ \hat{\mathfrak{G}}_{1\zeta_{\mathbb{R}}}(a) = \mathcal{L}_{1\zeta}, \\ \hat{\mathfrak{G}}_{2\zeta_{\mathbb{R}}}(a) = \mathcal{L}_{2\zeta}. \end{cases}$$
(31)

Subtracting (31) from Process i - Situation 1, one has

$$\begin{cases} \varepsilon'_{1\zeta_{n}}(\xi) = \mathsf{E}_{1\zeta_{n}}(\xi, \varepsilon_{1\zeta_{n}}(\xi), \varepsilon_{2\zeta_{n}}(\xi)), \\ \varepsilon'_{2\zeta_{n}}(\xi) = \mathsf{E}_{2\zeta_{n}}(\xi, \varepsilon_{1\zeta_{n}}(\xi), \varepsilon_{2\zeta_{n}}(\xi)), \\ \varepsilon_{1\zeta_{n}}(a) = 0, \\ \varepsilon_{2\zeta_{n}}(a) = 0, \end{cases}$$
(32)

wherein

$$\begin{cases} \mathsf{E}_{1\zeta_{\mathrm{II}}}(\xi, \varepsilon_{1\zeta_{\mathrm{II}}}(\xi), \varepsilon_{2\zeta_{\mathrm{II}}}(\xi)) = \mathsf{E}_{1\zeta}(\xi, \mathfrak{H}_{1\zeta}(\xi), \mathfrak{H}_{2\zeta}(\xi)) \\ -\mathsf{E}_{1\zeta_{\mathrm{II}}}(\xi, \mathfrak{H}_{1\zeta_{\mathrm{II}}}(\xi), \mathfrak{H}_{2\zeta_{\mathrm{II}}}(\xi)), \\ \mathsf{E}_{2\zeta_{\mathrm{II}}}(\xi, \varepsilon_{1\zeta_{\mathrm{II}}}(\xi), \varepsilon_{2\zeta_{\mathrm{II}}}(\xi)) = \mathsf{E}_{2\zeta}(\xi, \mathfrak{H}_{1\zeta}(\xi), \mathfrak{H}_{2\zeta}(\xi)) \\ -\mathsf{E}_{2\zeta_{\mathrm{II}}}(\xi, \mathfrak{H}_{1\zeta_{\mathrm{II}}}(\xi), \mathfrak{H}_{2\zeta_{\mathrm{II}}}(\xi)). \end{cases} \tag{33}$$

To solve (32), we can utilize LOP-GS. Then, we have an algebraic set of 2m transcendental equations. By handling this set, we get the required approximation.

6. The LOP-GS algorithm and solvability experiments

For the LOP-GS, the series formations and a new version of recurrence relations have been used to solve FTDMs controlled with FTICs. The LOPs are tested throughout the GS to show that they allow analytical and approximate solutions using a few terms of the LOPs.

Numerical methods have become indispensable tools for scientists and engineers, solving complex problems that often lack analytical counterparts like FTDMs. Algorithm 2 aims to develop the LOP-GS as a novel tactic for solving (1) and (2) using their ζ -cut formations. The

$$\left\langle \begin{bmatrix} \mathbf{z}_{1\zeta}(\xi) \\ \mathbf{z}_{2\zeta}(\xi) \end{bmatrix} - \begin{bmatrix} \mathfrak{F}_{1\zeta}(\xi) \\ \mathfrak{F}_{2\zeta}(\xi) \end{bmatrix}, \begin{bmatrix} \boldsymbol{\phi}_{1\zeta_{i}}(\xi) \\ \boldsymbol{\phi}_{2\zeta_{i}}(\xi) \end{bmatrix} \right\rangle = \left\langle \begin{bmatrix} \mathbf{z}_{1\zeta}(\xi) \\ \mathbf{z}_{2\zeta}(\xi) \end{bmatrix}, \begin{bmatrix} \boldsymbol{\phi}_{1\zeta_{i}}(\xi) \\ \boldsymbol{\phi}_{2\zeta_{i}}(\xi) \end{bmatrix} \right\rangle - \left\langle \begin{bmatrix} \mathfrak{F}_{1\zeta_{i}}(\xi) \\ \mathfrak{F}_{2\zeta_{i}}(\xi) \end{bmatrix}, \begin{bmatrix} \boldsymbol{\phi}_{1\zeta_{i}}(\xi) \\ \boldsymbol{\phi}_{2\zeta_{i}}(\xi) \end{bmatrix} \right\rangle \\
= \lim_{n \to \infty} \left\langle \begin{bmatrix} \mathfrak{F}_{1\zeta_{n}}(\xi) \\ \mathfrak{F}_{2\zeta_{n}}(\xi) \end{bmatrix}, \begin{bmatrix} \boldsymbol{\phi}_{1\zeta_{i}}(\xi) \\ \boldsymbol{\phi}_{2\zeta_{i}}(\xi) \end{bmatrix} \right\rangle - \begin{bmatrix} c_{i} \\ d_{i} \end{bmatrix} \\
= \begin{bmatrix} c_{i} \\ d_{i} \end{bmatrix} - \begin{bmatrix} c_{i} \\ d_{i} \end{bmatrix} \\
= \begin{bmatrix} 0 \\ 0 \end{bmatrix}.$$
(30)

$$\begin{split} \text{Hence,} \quad & \begin{bmatrix} z_{1\zeta}(\xi) \\ z_{2\zeta}(\xi) \end{bmatrix} = \begin{bmatrix} \mathfrak{G}_{1\zeta}(\xi) \\ \mathfrak{G}_{2\zeta}(\xi) \end{bmatrix} \quad \text{and} \quad \begin{bmatrix} \mathfrak{G}_{1\zeta\pi}(\xi) \\ \mathfrak{G}_{2\zeta\pi}(\xi) \end{bmatrix} = \begin{bmatrix} \sum_{i=0}^n c_i \phi_{1\zeta^i}(\xi) \\ \sum_{i=0}^n d_i \phi_{2\zeta^i}(\xi) \end{bmatrix} \\ \text{converges to } & \mathfrak{G}_{\zeta}(\xi) = \begin{bmatrix} \mathfrak{G}_{1\zeta}(\xi) \\ \mathfrak{G}_{2\zeta}(\xi) \end{bmatrix} \text{ as } & \mathbb{R} \to \infty. \end{split}$$

Theorem 6. Presume $\mathfrak{H}_{1\zeta}(\xi)$ and $\mathfrak{H}_{2\zeta}(\xi)$ are the exact solutions of CTICs, and $\mathfrak{H}_{1\zeta_{\mathbb{R}}}(\xi)$ and $\mathfrak{H}_{2\zeta_{\mathbb{R}}}(\xi)$ are their approximations. Then $\varepsilon_{1\zeta_{\mathbb{R}}}(\xi) = \mathfrak{H}_{1\zeta}(\xi) - \mathfrak{H}_{1\zeta_{\mathbb{R}}}(\xi)$ and $\varepsilon_{2\zeta_{\mathbb{R}}}(\xi) = \mathfrak{H}_{2\zeta}(\xi) - \mathfrak{H}_{2\zeta_{\mathbb{R}}}(\xi)$ can be approximated using the LOP-GS.

Proof. Herein $\mathfrak{H}_{1\zeta_{\mathbb{R}}}(\xi)$ and $\mathfrak{H}_{2\zeta_{\mathbb{R}}}(\xi)$ satisfy (23) with

resulting set will consist of two CTDMs for each SGD type, but to minimize the length of this essay and avoid repetition, we will review only the 1st case concerning the (1)-SGD since the remaining case is similar. Herein, all the symbolic computations have been performed using MATHEMATICA 11.

To elucidate further, CTDM can be proficiently characterized as FTDM. The next SRIC substantiates this claim (see Fig. 1, where resistance, solenoid, and voltage are denoted as R, L, \mathscr{E} , simultaneously):

$$\begin{cases} \mathscr{I}(\xi) = -\frac{R}{L}\mathscr{I}(\xi) + \mathscr{E}(\xi), \\ \mathscr{I}(0) \cong \frac{\mathscr{E}(0)}{R}. \end{cases}$$
 (34)

However, it is crucial to acknowledge that uncertainty in the (34)

may stem from natural influences, leakage, inaccuracies in element modeling, and electrical noise.

The SRIC involves a resistor and an inductor connected in series. The inductor resists changes in current, while the resistor controls the flow of current. This individual configuration is widely used in electronic devices and demands a detailed analysis of power distribution, impedance, voltage, and current. This framework allows for the analysis and calculation of key SRIC specifications, like transient behaviors, time constants, and current response.

Within (34), $\mathscr{I}(0)\cong\frac{\mathscr{E}(0)}{R}$ indicates that the initial current passing the inductor is approximately $\frac{\mathscr{E}(0)}{R}$ amperes, though not exactly $\frac{\mathscr{E}(0)}{R}$. This uncertainty can be attributed to several factors, including:

- Measurement error: accurately measuring the initial current in an inductor is a significant challenge due to inherent limitations in precision. This difficulty arises from the fact that the current through an inductor experiences rapid temporal fluctuations, where even small measurement errors can cause significant inaccuracies in the determined initial current.
- Model shape: the simplified version of (34) approximates the actual SRIC in real-world conditions. To illustrate, the model may overlook the fallout of parasitic resistance and capacitance within the SRIC, leading to some degree of uncertainty.
- Numerical inaccuracies: given the inherent limitations in computational precision, a certain degree of error is unavoidable when numerically solving (34).

The variability in $\frac{Z(0)}{R}$ in (34) can significantly impact its resolution. A slight deviation in $\frac{Z(0)}{R}$ may produce substantial differences in the predicted current when solving SRIC. Thus, acknowledging this uncertainty is crucial. To address it, two approaches are common:

- 1. Sensitivity analysis: evaluating how changes in $\mathscr{I}(0)$ affect the solution by solving (34) for different $\frac{\mathscr{E}(0)}{R}$ values.
- 2. Probabilistic approach: entrusting a probability distribution to $\frac{\mathcal{E}(0)}{R}$ and applying Monte-Carlo simulations to generate multiple realizations, forming a probability distribution of future values.

Applying fuzzification to (34) while accounting for the environment's stochastic nature enhances result accuracy and improves the detection of new constraints in circuit assessment, as exhibited next.

Application 1. Let's analyze the SRIC subject to some uncertainty

$$\mathscr{I}(\xi) = -\frac{R}{L}\mathscr{I}(\xi) + \mathscr{E}(\xi), \ \xi \in [0,1], \tag{35}$$

controlled by the FTIC

$$\mathscr{I}(0) = \mathscr{L} \text{ with } \mathscr{L}(\kappa) = \begin{cases} 25\kappa - 24, \ 0.96 \le \kappa \le 1, \\ -100\kappa + 101, \ 1 \le \kappa \le 1.01. \end{cases}$$
 (36)

The ζ -cut formation of (35) and (36) leads to

$$\left[\mathbf{E}(\xi, \mathscr{I}(\xi))\right]^{\zeta} = \left[-\frac{R}{L} \mathscr{I}_{2\zeta}(\xi), -\frac{R}{L} \mathscr{I}_{1\zeta}(\xi) \right] + \mathscr{E}(\xi). \tag{37}$$

$$[\mathcal{L}]^{\zeta} = [0.96 + 0.04\zeta, 1.01 - 0.01\zeta]. \tag{38}$$

Numerically, assume $(R,L)=(1,1)/({\rm Ohm},{\rm Henry})$ with $\mathscr{E}(\xi)=\sin(\xi)+1.$ Anyhow, to reveal the fuzzy solution of (35) and (36), consider two situations

Situation i. The CTDMs corresponding to type (1)-SGD are

$$\begin{cases} \mathscr{I}_{1\zeta}(\xi) = -\mathscr{I}_{2\zeta}(\xi) + \sin(\xi) + 1, \\ \mathscr{I}_{2\zeta}(\xi) = -\mathscr{I}_{1\zeta}(\xi) + \sin(\xi) + 1, \end{cases}$$
(39)

controlled by the CTICs

$$\begin{cases} \mathscr{I}_{1\zeta}(0) = \frac{24}{25} + \frac{1}{25}\zeta, \\ \mathscr{I}_{2\zeta}(0) = \frac{101}{100} - \frac{1}{100}\zeta. \end{cases} \tag{40}$$

Herein, the exact $\mathscr{I}_{1\zeta}(\xi)$ and $\mathscr{I}_{2\zeta}(\xi)$ of (39) and (40) is

$$\begin{cases} \mathscr{I}_{1\zeta}(\xi) = \frac{1}{2}(\sin(\xi) - \cos(\xi)) + \left(\frac{24}{25} + \frac{1}{25}\zeta\right) \cosh(\xi) \\ -\left(\frac{101}{100} - \frac{1}{100}\zeta\right) \sinh(\xi) - \frac{1}{2}e^{-\xi} + 1, \end{cases}$$

$$\mathscr{I}_{2\zeta}(\xi) = \frac{1}{2}(\sin(\xi) - \cos(\xi)) + \left(\frac{101}{100} - \frac{1}{100}\zeta\right) \cosh(\xi)$$

$$-\left(\frac{24}{25} + \frac{1}{25}\zeta\right) \sinh(\xi) - \frac{1}{2}e^{-\xi} + 1.$$

$$(41)$$

Situation ii. The CTDMs corresponding to type (2)-SGD are

$$\begin{cases} \mathscr{I}_{1\zeta}(\xi) = -\mathscr{I}_{1\zeta}(\xi) + \sin(\xi) + 1, \\ \mathscr{I}_{2\zeta}(\xi) = -\mathscr{I}_{2\zeta}(\xi) + \sin(\xi) + 1, \end{cases}$$

$$\tag{42}$$

controlled by the CTICs

$$\begin{cases} \mathscr{I}_{1\zeta}(0) = \frac{24}{25} + \frac{1}{25}\zeta, \\ \mathscr{I}_{2\zeta}(0) = \frac{101}{100} - \frac{1}{100}\zeta. \end{cases}$$
 (43)

Herein, the exact $\mathcal{I}_{1\zeta}(\xi)$ and $\mathcal{I}_{2\zeta}(\xi)$ of (42) and (43) are

$$\begin{cases} \mathscr{I}_{1\zeta}(\xi) = -\frac{1}{2}e^{-\xi} + \left(\frac{24}{25} + \frac{1}{25}\zeta\right)e^{-\xi} + 1 + \frac{1}{2}(\sin(\xi) - \cos(\xi)), \\ \mathscr{I}_{2\zeta}(\xi) = -\frac{1}{2}e^{-\xi} + \left(\frac{101}{100} - \frac{1}{100}\zeta\right)e^{-\xi} + 1 + \frac{1}{2}(\sin(\xi) - \cos(\xi)). \end{cases}$$
(44)

Application 2. Let's analyze the FTDM, including uncertain forcing and nonhomogeneous terms [11]

$$\mathfrak{S}'(\xi) = 2\xi\mathfrak{S}(\xi) + \xi\mathfrak{S}, \xi \in [0, 1],\tag{45}$$

controlled by the FTIC

$$\mathfrak{H}(0) = \mathscr{L} \text{ with } \mathscr{L}(\kappa) = \max(0, 1 - |\kappa|), \kappa \in \mathbb{R}. \tag{46}$$

The ζ -cut formation of (45) and (46) leads to

$$[\mathfrak{U}(\xi,\mathfrak{H}(\xi))]^{\zeta} = [2\xi\mathfrak{H}_{1\zeta}(\xi) + \xi(\zeta - 1), 2\xi\mathfrak{H}_{2\zeta}(\xi) + \xi(1 - \zeta)]. \tag{47}$$

$$[\mathscr{L}]^{\zeta} = [\zeta - 1, 1 - \zeta]. \tag{48}$$

Anyhow, to reveal the fuzzy solution of (45) and (46), consider two situations as

Situation i. The CTDMs corresponding to type (1)-SGD are

$$\begin{cases} \hat{\mathcal{G}}_{1\zeta}(\xi) = 2\xi \hat{\mathcal{G}}_{1\zeta}(\xi) + \xi(\zeta - 1), \\ \hat{\mathcal{G}}_{2\zeta}(\xi) = 2\xi \hat{\mathcal{G}}_{2\zeta}(\xi) + \xi(1 - \zeta), \end{cases}$$

$$(49)$$

controlled by the CTICs

$$\begin{cases}
\hat{\mathfrak{G}}_{1\zeta}(0) = \zeta - 1, \\
\hat{\mathfrak{D}}_{2\zeta}(0) = 1 - \zeta.
\end{cases}$$
(50)

Herein, the exact $\mathfrak{H}_{1\zeta}(\xi)$ and $\mathfrak{H}_{2\zeta}(\xi)$ of (49) and (50) are

Table 1 Results of Situation i in Application 1: |Error| in LOP-GS solutions for $\mathscr{I}_{1\zeta_n n}\left(\xi_{\frac{1}{2}}\right)$.

	$\zeta_0 = 0$	$\zeta_1 = 0.25$	$\zeta_3 = 0.5$	$\zeta_3 = 0.75$	$\zeta_4 = 1$
0	0	0	0	0	0
0.1	9.699959×10^{-9}	9.640032×10^{-9}	9.115334×10^{-9}	9.520181×10^{-9}	9.460254×10^{-9}
0.2	2.641258×10^{-8}	2.617179×10^{-8}	2.457983×10^{-8}	2.569021×10^{-8}	2.544942×10^{-8}
0.3	1.761498×10^{-8}	1.750937×10^{-8}	1.698563×10^{-8}	1.729814×10^{-8}	1.719253×10^{-8}
0.4	3.429775×10^{-8}	3.400601×10^{-8}	3.244489×10^{-8}	3.342254×10^{-8}	3.313080×10^{-8}
0.5	1.728345×10^{-9}	1.765390×10^{-9}	1.675457×10^{-9}	1.839485×10^{-9}	1.876531×10^{-9}
0.6	3.581515×10^{-8}	3.554604×10^{-8}	3.357486×10^{-8}	3.500782×10^{-8}	3.473871×10^{-8}
0.7	1.551620×10^{-8}	1.535626×10^{-8}	1.406268×10^{-8}	1.503639×10^{-8}	1.487646×10^{-8}
0.8	$2.921767 imes 10^{-8}$	2.901339×10^{-8}	2.816756×10^{-8}	2.860483×10^{-8}	2.840054×10^{-8}
0.9	8.831035×10^{-9}	8.742033×10^{-9}	8.759028×10^{-9}	8.564023×10^{-9}	8.475021×10^{-9}
1	1.076916×10^{-13}	1.081357×10^{-13}	6.510481×10^{-10}	1.028066×10^{-13}	$1.028066\ \times 10^{-13}$

$$\begin{cases} \mathfrak{S}_{1\zeta}(\xi) = \frac{1}{2} \left(3e^{\xi^2} - 1 \right) (\zeta - 1), \\ \mathfrak{S}_{2\zeta}(\xi) = \frac{1}{2} \left(3e^{\xi^2} - 1 \right) (1 - \zeta). \end{cases}$$

$$(51)$$

Situation ii. The CTDMs corresponding to type (2)-SGD are

$$\begin{cases} \hat{\mathcal{G}}_{1\zeta}'(\xi) = 2\xi \hat{\mathcal{G}}_{2\zeta}(\xi) + \xi(1-\zeta), \\ \hat{\mathcal{G}}_{2\zeta}'(\xi) = 2\xi \hat{\mathcal{G}}_{1\zeta}(\xi) + \xi(\zeta-1), \end{cases}$$
(52)

controlled by the CTICs

$$\begin{cases}
\hat{\mathfrak{D}}_{1\zeta}(0) = \zeta - 1, \\
\hat{\mathfrak{D}}_{2\zeta}(0) = 1 - \zeta.
\end{cases}$$
(53)

Herein, the exact $\mathfrak{H}_{1\zeta}(\xi)$ and $\mathfrak{H}_{2\zeta}(\xi)$ of (52) and (53) are

$$\begin{cases} \mathfrak{S}_{1\zeta}(\xi) = \frac{1}{2} \left(3e^{-\xi^2} - 1 \right) (\zeta - 1), \\ \mathfrak{S}_{2\zeta}(\xi) = \frac{1}{2} \left(3e^{-\xi^2} - 1 \right) (1 - \zeta). \end{cases}$$
 (54)

7. Findings and comparative analysis

This piece offers the key findings of the study and provides a comparative analysis to contextualize the results. By examining trends, patterns, and variations, we assess how the data aligns with existing literature, theoretical frameworks, or industry benchmarks. Through this analysis, we aim to identify significant insights, highlight similarities and differences, analyze and compare, and draw meaningful conclusions that contribute to a deeper understanding of the subject.

The discussions of Application 1 are as follows. To obtain the desired outcomes, we employ the LOP-GS to get the evolution values of the fuzzy solution at some values of ξ in [0,1] and ζ in the truth [0,1] interval, utilizing Algorithm 1 and Algorithm 2 within N=10 and M=4. Anyhow, Table 1 and Table 2 display |Error| in $\mathscr{I}_{1\zeta_{\eta}\pi}\left(\xi_{j}\right)$ and $\mathscr{I}_{2\zeta_{\eta}\pi}\left(\xi_{j}\right)$, comparing within $\mathscr{I}_{1\zeta_{\eta}}\left(\xi_{j}\right)$ and $\mathscr{I}_{2\zeta_{\eta}}\left(\xi_{j}\right)$, simultaneously, at $\pi=6$ in

Situation i. Tables 3 and 4 display similar results in Situation ii. The two shapes in Fig. 2 portray the fuzzy approximate solution $\left[\mathscr{F}_{\mathbb{R}}\left(\xi_{j}\right)\right]^{\zeta_{\eta}}$ in Situation i and Situation ii, simultaneously at $\mathbb{R}=6$.

The discussions of Application 2 are as follows. To obtain the desired outcomes, we employ the LOP-GS to get the evolution values of the fuzzy solution at some values of ξ in [0,1] and ζ in the truth [0,1] interval, utilizing Algorithm 1 and Algorithm 2 within N=10 and M=4. Anyhow, Table 5 and Table 6 display |Error| in $\mathfrak{H}_{1\zeta_\eta}(\xi_{\mathfrak{f}})$ and $\mathfrak{H}_{2\zeta_\eta}(\xi_{\mathfrak{f}})$ comparing within $\mathfrak{H}_{1\zeta_\eta}(\xi_{\mathfrak{f}})$ and $\mathfrak{H}_{2\zeta_\eta}(\xi_{\mathfrak{f}})$, simultaneously, at $\mathfrak{H}=6$ in Situation i. Tables 7 and 8 display similar results in Situation ii. The two shapes in Fig. 3 portray the fuzzy approximate solution $[\mathfrak{H}_{\mathfrak{H}}(\xi)]^{\zeta_\eta}$ in Situation i and Situation ii, simultaneously at $\mathfrak{H}=6$.

The figures clearly show that $\forall \xi_{i} \in [0,1]$ and $\forall \zeta_{\eta} \in [0,1]$, the ζ -cut formation of the LOP-GS approximations corresponds to valid level sets. These findings align with Situation 1 and Situation 2 of Algorithm 1. Also, it is evident that the graphs closely align, exhibiting similar behavior and strong agreement. Notably, the FTDM significantly influences the model profiles, often resulting in unconventional behavior when deviating substantially from the crisp value.

Next, we compare the gained LOP-GS results with those HKS results that were studied in [11]. Such comparisons are important because they help us understand how well the LOP-GS performs in practice. These results also give readers more confidence in the proposed approach, as they show how it stands relative to trusted techniques that have already been studied and used by other researchers. Anyhow, results of LOP-GS against HKS in |Error| even nodals of Application 1 at some values of ξ in [0, 1] and ζ in truth [0, 1] interval are tabulated in Tables 9–12. Similarly, Tables 9–12 show the comparative results for Application 2.

Table 13, 14, 15, 16

In comparative terminologies, the LOP-GS solves Application 1 more accurately from HKS at all nodal ξ_j in [0,1] and ζ_η in truth [0,1] interval, whilst for Application 2, the LOP-GS closely and better than the HKS in some nodal ξ_j in [0,1] and ζ in truth [0,1] interval, especially at $\xi_j=1$, and the |Error| between LOP-GS and HKS nodals is equal at $\zeta_\eta=1$. The su-

Table 2 Results of Situation i in Application 1: |Error| in LOP-GS solutions for $\mathscr{I}_{2\zeta_y n}\left(\xi_j\right)$.

	$\zeta_0 = 0$	$\zeta_1 = 0.25$	$\zeta_3 = 0.5$	$\zeta_3 = 0.75$	$\zeta_4 = 1$
0	0	0	0	0	0
0.1	8.959909×10^{-9}	9.060611×10^{-9}	9.008478×10^{-9}	9.264671×10^{-9}	9.460254×10^{-9}
0.2	2.393753×10^{-8}	2.430009×10^{-8}	2.391514×10^{-8}	2.500283×10^{-8}	2.544942×10^{-8}
0.3	1.650490×10^{-8}	1.668440×10^{-8}	1.614883×10^{-8}	1.709092×10^{-8}	1.719253×10^{-8}
0.4	3.142851×10^{-8}	3.185510×10^{-8}	2.995948×10^{-8}	3.278096×10^{-8}	$3.313080\ \times 10^{-8}$
0.5	1.873253×10^{-9}	1.878247×10^{-9}	1.495614×10^{-9}	1.790433×10^{-9}	1.876531×10^{-9}
0.6	3.289200×10^{-8}	3.336146×10^{-8}	2.887614×10^{-8}	3.417750×10^{-8}	3.473871×10^{-8}
0.7	1.382819×10^{-8}	1.409980×10^{-8}	1.162755×10^{-8}	1.449501×10^{-8}	1.487646×10^{-8}
0.8	2.723790×10^{-8}	2.751953×10^{-8}	2.236517×10^{-8}	2.825590×10^{-8}	2.840054×10^{-8}
0.9	8.206561×10^{-9}	8.267845×10^{-9}	6.676907×10^{-9}	8.588783×10^{-9}	8.475021×10^{-9}
1	2.997042×10^{-10}	2.253783×10^{-10}	4.766986×10^{-10}	$3.006019 imes 10^{-10}$	$1.028066\ \times 10^{-13}$

 Table 3

 Results of Situation ii in Application 1: |Error| in LOP-GS solutions for $\mathscr{I}_{1\xi_{\eta^n}}(\xi_{\bar{\jmath}})$.

	$\zeta_0 = 0$	$\zeta_1 = 0.25$	$\zeta_3 = 0.5$	$\zeta_3 = 0.75$	$\zeta_4 = 1$
0	0	0	0	0	0
0.1	9.207106×10^{-9}	9.270260×10^{-9}	9.333512×10^{-9}	9.396765×10^{-9}	9.460018×10^{-9}
0.2	$2.481272\ \times 10^{-8}$	2.497259×10^{-8}	2.513188×10^{-8}	2.529118×10^{-8}	2.545047×10^{-8}
0.3	1.673867×10^{-8}	1.685172×10^{-8}	1.696510×10^{-8}	1.707848×10^{-8}	1.719186×10^{-8}
0.4	3.230559×10^{-8}	3.251236×10^{-8}	3.271872×10^{-8}	3.292508×10^{-8}	3.313144×10^{-8}
0.5	1.804567×10^{-9}	1.821704×10^{-9}	1.839559×10^{-9}	1.857414×10^{-9}	1.875268×10^{-9}
0.6	3.386938×10^{-8}	3.408641×10^{-8}	3.430367×10^{-8}	3.452093×10^{-8}	3.473819×10^{-8}
0.7	1.452796×10^{-8}	1.461569×10^{-8}	1.470288×10^{-8}	1.479007×10^{-8}	1.487727×10^{-8}
0.8	$2.769257 imes 10^{-8}$	2.786881×10^{-8}	2.804569×10^{-8}	2.822258×10^{-8}	2.839946×10^{-8}
0.9	8.278173×10^{-9}	8.327643×10^{-9}	8.376879×10^{-9}	8.426116×10^{-9}	8.475353×10^{-9}
1	1.063593×10^{-13}	9.681144×10^{-14}	9.747758×10^{-14}	9.814371×10^{-14}	9.880984×10^{-14}

Table 4 Results of Situation ii in Application 1: |Error| in LOP-GS solutions for $\mathscr{S}_{2\zeta_\eta n}\left(\xi_j\right)$.

	$\zeta_0 = 0$	$\zeta_1=0.25$	$\zeta_3 = 0.5$	$\zeta_3 = 0.75$	$\zeta_4 = 1$
0	0	0	0	0	0
0.1	9.523382×10^{-9}	9.508021×10^{-9}	9.492207×10^{-9}	9.476393×10^{-9}	9.460018×10^{-9}
0.2	2.560914×10^{-8}	2.556715×10^{-8}	2.552733×10^{-8}	2.548752×10^{-8}	$2.545047\ \times 10^{-8}$
0.3	1.730560×10^{-8}	1.727862×10^{-8}	1.725027×10^{-8}	1.722193×10^{-8}	1.719186×10^{-8}
0.4	3.333737×10^{-8}	3.328444×10^{-8}	3.323285×10^{-8}	3.318127×10^{-8}	3.313144×10^{-8}
0.5	1.893882×10^{-9}	1.892070×10^{-9}	1.887599×10^{-9}	1.883128×10^{-9}	1.875268×10^{-9}
0.6	3.495572×10^{-8}	3.490251×10^{-8}	3.484819×10^{-8}	3.479387×10^{-8}	3.473819×10^{-8}
0.7	1.496391×10^{-8}	1.494045×10^{-8}	1.491866×10^{-8}	1.489686×10^{-8}	$1.487727\ \times 10^{-8}$
0.8	2.857702×10^{-8}	2.853505×10^{-8}	2.849083×10^{-8}	2.844660×10^{-8}	2.839946×10^{-8}
0.9	8.524350×10^{-9}	8.511395×10^{-9}	8.499088×10^{-9}	8.486781×10^{-9}	8.475353×10^{-9}
1	1.081357×10^{-13}	1.085798×10^{-13}	1.088018×10^{-13}	1.083577×10^{-13}	9.880984×10^{-14}

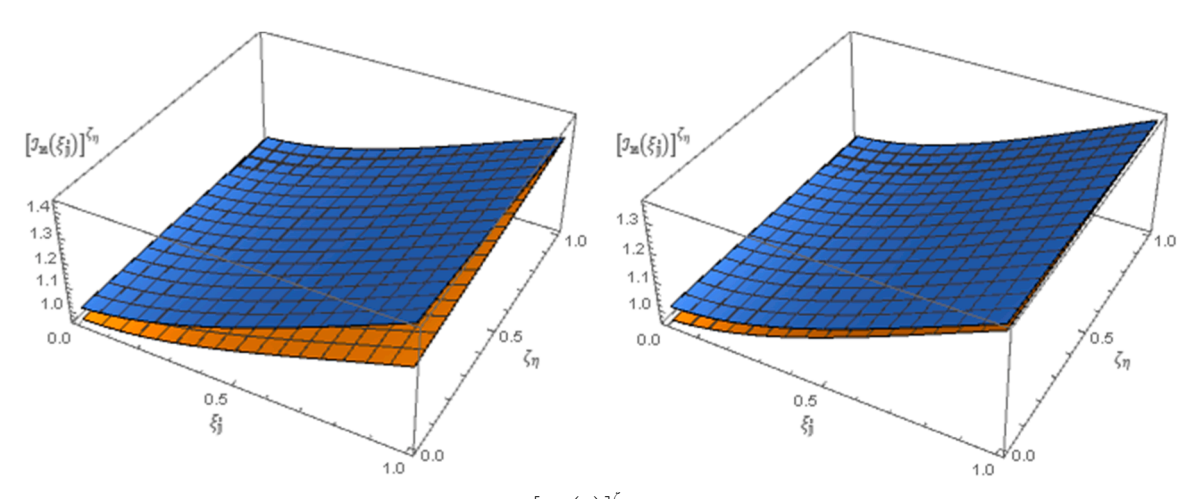


Fig. 2. Portrayal of Application 1: the fuzzy approximate solution $\left[\mathscr{I}_{n}\left(\xi_{j}\right)\right]^{\zeta_{\eta}}$ in Situation 1 and Situation 2, simultaneously as: blue: $\mathscr{I}_{1\zeta_{\eta}n}\left(\xi_{j}\right)$ and brown: $\mathscr{I}_{2\zeta_{\eta}n}\left(\xi_{j}\right)$.

 Table 5

 Results of Situation i in Application 2: |Error| in LOP-GS solutions for $\mathfrak{F}_{1\zeta_{\eta^n}}(\xi_j)$.

	$\zeta_0 = 0$	$\zeta_1 = 0.25$	$\zeta_3 = 0.5$	$\zeta_3 = 0.75$	$\zeta_4=1$
0	0	0	0	0	0
0.1	1.988820×10^{-5}	1.491615×10^{-5}	9.944103×10^{-6}	4.972051×10^{-6}	0
0.2	8.403361×10^{-5}	6.302520×10^{-5}	4.201680×10^{-5}	2.100840×10^{-5}	0
0.3	3.484081×10^{-5}	2.613060×10^{-5}	1.742040×10^{-5}	8.710202×10^{-6}	0
0.4	1.083038×10^{-4}	$8.122787\ \times 10^{-5}$	5.415191×10^{-5}	$2.707595\ \times 10^{-5}$	0
0.5	2.142255×10^{-4}	1.606691×10^{-5}	1.071128×10^{-5}	5.355639×10^{-6}	0
0.6	9.981814×10^{-5}	7.486361×10^{-5}	4.990907×10^{-5}	2.495453×10^{-5}	0
0.7	7.024598×10^{-4}	5.268448×10^{-5}	3.512299×10^{-5}	1.756149×10^{-5}	0
0.8	7.547951×10^{-4}	5.660963×10^{-5}	3.773975×10^{-5}	1.886987×10^{-5}	0
0.9	4.172766×10^{-5}	3.129574×10^{-5}	2.086383×10^{-5}	1.043191×10^{-5}	0
1	2.894884×10^{-8}	2.171133×10^{-8}	$1.447422 imes 10^{-8}$	7.237113×10^{-9}	0

 $\begin{tabular}{l} \textbf{Table 6} \\ \textbf{Results of Situation i in Application 2: } | \textbf{Error}| \ \textbf{in LOP-GS solutions for } \mathfrak{S}_{2\zeta_{\eta^n}}\Big(\xi_{\hat{\jmath}}\Big). \end{tabular}$

	$\zeta_0 = 0$	$\zeta_1=0.25$	$\zeta_3=0.5$	$\zeta_3 = 0.75$	$\zeta_4 = 1$
0	0	0	0	0	0
0.1	1.988820×10^{-5}	1.491615×10^{-5}	9.944103×10^{-6}	4.972051×10^{-6}	0
0.2	8.403361×10^{-5}	6.302520×10^{-5}	4.201680×10^{-5}	$2.100842\ imes 10^{-5}$	0
0.3	3.484081×10^{-5}	2.613060×10^{-5}	1742040×10^{-5}	8.710203×10^{-6}	0
0.4	1.083038×10^{-4}	8.122787×10^{-5}	5.415191×10^{-5}	2.707595×10^{-5}	0
0.5	$2.142255\ \times 10^{-5}$	1.606691×10^{-5}	$1.071127\ \times 10^{-5}$	5.355639×10^{-6}	0
0.6	9.981814×10^{-5}	7.486361×10^{-5}	4.990907×10^{-5}	2.495453×10^{-5}	0
0.7	7.024598×10^{-5}	5.268448×10^{-5}	3.512299×10^{-5}	1.756149×10^{-5}	0
0.8	7.549516×10^{-5}	5.660963×10^{-5}	3.773975×10^{-5}	1.886987×10^{-5}	0
0.9	4.172766×10^{-5}	3.129574×10^{-5}	2.086383×10^{-5}	1.043191×10^{-5}	0
1	2.894884×10^{-8}	2.171159×10^{-8}	1.447440×10^{-8}	7.237200×10^{-9}	0

 Table 7

 Results of Situation ii in Application 2: |Error| in LOP-GS solutions for $\mathfrak{F}_{1\zeta_{\eta^n}}(\xi_j)$.

	$\zeta_0 = 0$	$\zeta_1=0.25$	$\zeta_3=0.5$	$\zeta_3=0.75$	$\zeta_4 = 1$
0	0.0	0.0	0.0	0.0	0
0.1	4.740907×10^{-6}	3.555680×10^{-6}	2.370453×10^{-6}	1.185226×10^{-6}	0
0.2	1.286366×10^{-5}	9.647746×10^{-6}	6.431831×10^{-6}	3.215915×10^{-6}	0
0.3	8.758031×10^{-6}	6.568523×10^{-6}	4.379015×10^{-6}	2.189507×10^{-6}	0
0.4	1.604316×10^{-5}	1.203237×10^{-5}	8.021582×10^{-6}	4.010791×10^{-6}	0
0.5	1.747763×10^{-6}	1.310822×10^{-6}	8.738819×10^{-7}	4.369409×10^{-7}	0
0.6	1.681086×10^{-5}	1.260815×10^{-5}	8.405434×10^{-6}	4.202717×10^{-6}	0
0.7	5.882519×10^{-6}	4.411889×10^{-6}	2.941259×10^{-6}	1.470629×10^{-6}	0
0.8	1.399371×10^{-5}	1.049528×10^{-5}	6.996856×10^{-6}	3.498428×10^{-6}	0
0.9	3.007249×10^{-6}	$2.255437 imes 10^{-6}$	1.503624×10^{-6}	7.518123×10^{-7}	0
1	$1.510512\ imes 10^{-8}$	1.132884×10^{-8}	7.552561×10^{-9}	3.776281×10^{-9}	0

Table 8 Results of Situation 2 in Application 2: |Error| in LOP-GS solutions for $\mathfrak{G}_{2\zeta_{\eta^n}}\left(\xi_{\hat{\jmath}}\right)$.

	$\zeta_0 = 0$	$\zeta_1 = 0.25$	$\zeta_3 = 0.5$	$\zeta_3 = 0.75$	$\zeta_4 = 1$
0	0	0	0	0	0
0.1	4.740958×10^{-6}	3.555718×10^{-6}	$2.370479 imes 10^{-6}$	1.185239×10^{-6}	0
0.2	1.286359×10^{-5}	9.647697×10^{-6}	6.431798×10^{-6}	3.215899×10^{-6}	0
0.3	8.758153×10^{-6}	$6.568615 imes 10^{-6}$	4.379076×10^{-6}	$2.189538 imes 10^{-6}$	0
0.4	1.604330×10^{-5}	$1.203247 imes 10^{-5}$	8.021651×10^{-6}	$4.010825 imes 10^{-6}$	0
0.5	1.747600×10^{-6}	$1.310700 imes 10^{-6}$	8.738000×10^{-7}	4.369000×10^{-7}	0
0.6	1.681063×10^{-5}	$1.260797 imes 10^{-5}$	8.405316×10^{-6}	4.202658×10^{-6}	0
0.7	5.882188×10^{-6}	4.411641×10^{-6}	2.941094×10^{-6}	$1.470547 imes 10^{-6}$	0
0.8	1.399411×10^{-5}	$1.049558 imes 10^{-5}$	6.997057×10^{-6}	3.498528×10^{-6}	0
0.9	3.007663×10^{-6}	$2.255747 imes 10^{-6}$	1.503831×10^{-6}	7.519159×10^{-7}	0
1	1.556218×10^{-8}	1.167163×10^{-8}	$7.781090\ \times 10^{-9}$	3.890545×10^{-9}	0

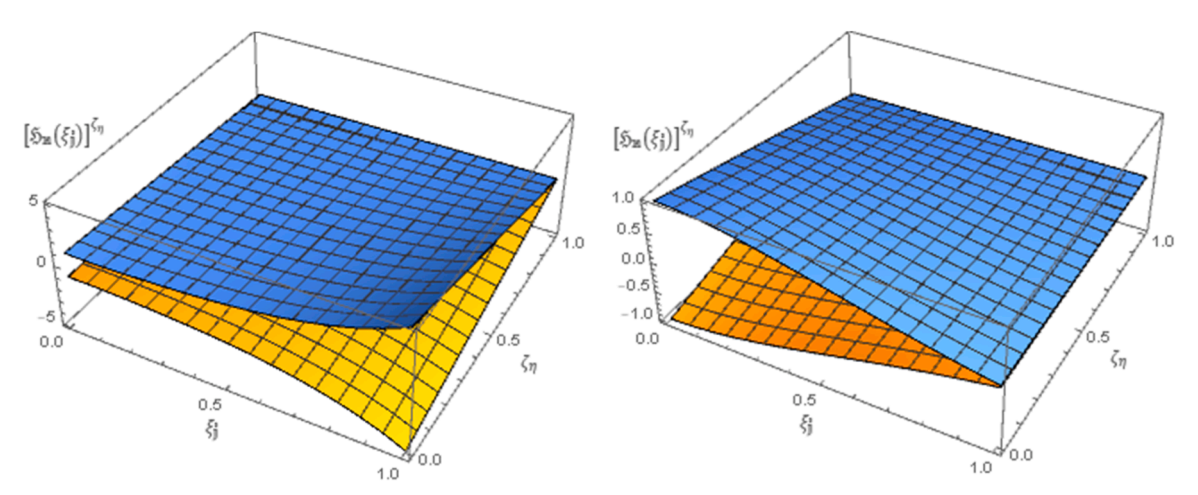


Fig. 3. Portrayal of LOP-GS in Application 2: the fuzzy approximate solution $\left[\mathfrak{F}_{n}\left(\xi_{j}\right)\right]^{\zeta_{\eta}}$ in Situation 1 and Situation 2, simultaneously as: blue: $\mathfrak{F}_{1\zeta_{\eta}n}\left(\xi_{j}\right)$ and brown: $\mathfrak{F}_{2\zeta_{\eta}n}\left(\xi_{j}\right)$.

 $\textbf{Table 9} \\ \textbf{Results of LOP-GS against HKS in } |\textbf{Error}| \ \textbf{even nodal of Situation i in Application 1 for } \mathcal{I}_{1\zeta_{\eta}n}\left(\xi_{\hat{j}}\right).$

	Strategy	$\zeta_0 = 0$	$\zeta_1 = 0.25$	$\zeta_3 = 0.5$	$\zeta_3 = 0.75$	$\zeta_4=1$
0.2	LOP-GS	2.6412×10^{-8}	2.6171×10^{-8}	2.4579×10^{-8}	2.5690×10^{-8}	2.5449×10^{-8}
	HKS	1.8936×10^{-6}	1.8901×10^{-6}	1.6267×10^{-6}	1.4144×10^{-6}	5.2914×10^{-7}
0.4	LOP-GS	3.4297×10^{-8}	3.4006×10^{-8}	3.2444×10^{-8}	$3.3422 imes 10^{-8}$	3.3130×10^{-8}
	HKS	3.6294×10^{-6}	3.6203×10^{-6}	3.1138×10^{-6}	2.7056×10^{-6}	9.5426×10^{-7}
0.6	LOP-GS	$3.5815 imes 10^{-8}$	3.5546×10^{-8}	3.3574×10^{-8}	3.5007×10^{-8}	3.4738×10^{-8}
	HKS	5.2279×10^{-6}	5.2109×10^{-6}	4.4784×10^{-6}	3.8884×10^{-6}	1.3071×10^{-6}
0.8	LOP-GS	$2.9217 imes 10^{-8}$	2.9013×10^{-8}	2.8167×10^{-8}	2.8604×10^{-8}	2.8400×10^{-8}
	HKS	6.6997×10^{-6}	6.6721×10^{-6}	5.7292×10^{-6}	4.9700×10^{-6}	1.6089×10^{-6}
1	LOP-GS	1.0769×10^{-13}	1.0813×10^{-13}	6.5104×10^{-10}	1.0280×10^{-13}	1.0280×10^{-13}
	HKS	$8.0485 imes 10^{-6}$	$8.0072\ \times 10^{-6}$	6.8686×10^{-6}	$5.9523\ \times 10^{-6}$	$1.8732\ \times 10^{-6}$

 Table 10

 Results of LOP-GS against HKS in |Error| even nodal of Situation i in Application 1 for $\mathscr{I}_{2\zeta_{\eta}\pi}\left(\xi_{\bar{j}}\right)$.

	Strategy	$\zeta_0 = 0$	$\zeta_1=0.25$	$\zeta_3 = 0.5$	$\zeta_3 = 0.75$	$\zeta_4 = 1$
0.2	LOP-GS	2.3937×10^{-8}	2.4300×10^{-8}	2.3915×10^{-8}	2.5002×10^{-8}	2.5449×10^{-8}
	HKS	1.8390×10^{-6}	1.8491×10^{-6}	1.6032×10^{-6}	1.4042×10^{-6}	5.2914×10^{-7}
0.4	LOP-GS	3.1428×10^{-8}	3.1855×10^{-8}	2.99594×10^{-8}	3.2780×10^{-8}	$3.3130 \ \times 10^{-8}$
	HKS	3.5081×10^{-6}	3.5294×10^{-6}	3.06156×10^{-6}	2.6829×10^{-6}	9.5426×10^{-7}
0.6	LOP-GS	3.2892×10^{-8}	3.33614×10^{-8}	2.8876×10^{-8}	3.4177×10^{-8}	3.4738×10^{-8}
	HKS	5.0252×10^{-6}	5.0589×10^{-6}	4.3910×10^{-6}	3.8503×10^{-6}	1.3071×10^{-6}
0.8	LOP-GS	2.7237×10^{-8}	2.7519×10^{-8}	2.2365×10^{-8}	2.8255×10^{-8}	$2.8400 \ \times 10^{-8}$
	HKS	6.3976×10^{-6}	6.4455×10^{-6}	5.5989×10^{-6}	4.9133×10^{-6}	1.6089×10^{-6}
1	LOP-GS	2.9970×10^{-10}	2.2537×10^{-10}	4.7669×10^{-10}	3.0060×10^{-10}	1.0280×10^{-13}
	HKS	7.6248×10^{-6}	7.6895×10^{-6}	6.6859×10^{-6}	5.8728×10^{-6}	1.8732×10^{-6}

 Table 11

 Results of LOP-GS against HKS in |Error| even nodal of Situation ii in Application 1 for $\mathscr{S}_{2\zeta_{\eta^n}}(\xi_{\hat{\jmath}})$.

	Strategy	$\zeta_0 = 0$	$\zeta_1 = 0.25$	$\zeta_3 = 0.5$	$\zeta_3 = 0.75$	$\zeta_4=1$
0.2	LOP-GS	2.4812×10^{-8}	2.4972×10^{-8}	2.5131×10^{-8}	2.5291×10^{-8}	2.5450×10^{-8}
	HKS	5.1903×10^{-7}	5.2156×10^{-7}	5.2409×10^{-7}	5.2662×10^{-7}	5.2914×10^{-7}
0.4	LOP-GS	3.2305×10^{-8}	3.2512×10^{-8}	3.2718×10^{-8}	3.2925×10^{-8}	3.3131×10^{-8}
	HKS	9.3851×10^{-7}	9.4245×10^{-7}	9.4638×10^{-7}	9.5032×10^{-7}	9.5426×10^{-7}
0.6	LOP-GS	3.3869×10^{-8}	3.4086×10^{-8}	3.4303×10^{-8}	3.4520×10^{-8}	3.4738×10^{-8}
	HKS	1.2890×10^{-6}	1.2935×10^{-6}	1.2980×10^{-6}	1.3025×10^{-6}	1.3071×10^{-6}
0.8	LOP-GS	2.7692×10^{-8}	2.7868×10^{-8}	2.8045×10^{-8}	2.8222×10^{-8}	2.8399×10^{-8}
	HKS	1.5912×10^{-6}	1.5956×10^{-6}	1.6000×10^{-6}	1.6044×10^{-6}	1.6089×10^{-6}
1	LOP-GS	1.0635×10^{-13}	9.6811×10^{-14}	9.7477×10^{-14}	9.8143×10^{-14}	9.8809×10^{-14}
	HKS	1.8578×10^{-6}	1.8616×10^{-6}	1.8655×10^{-6}	1.8694×10^{-6}	1.8732×10^{-6}

 Table 12

 Results of LOP-GS against HKS in |Error| even nodal of Situation ii in Application 1 for $\mathscr{I}_{2\zeta_\eta n}\left(\xi_j\right)$.

	Strategy	$\zeta_0 = 0$	$\zeta_1 = 0.25$	$\zeta_3 = 0.5$	$\zeta_3 = 0.75$	$\zeta_4 = 1$
0.2	LOP-GS	2.5609×10^{-8}	2.5567×10^{-8}	2.5527×10^{-8}	2.5487×10^{-8}	2.5450×10^{-8}
	HKS	5.3167×10^{-7}	5.3104×10^{-7}	5.3041×10^{-7}	5.2978×10^{-7}	5.2914×10^{-7}
0.4	LOP-GS	3.3337×10^{-8}	3.3284×10^{-8}	$3.3232 imes 10^{-8}$	3.3181×10^{-8}	3.3131×10^{-8}
	HKS	9.5819×10^{-7}	9.5721×10^{-7}	9.5622×10^{-7}	9.5524×10^{-7}	9.5426×10^{-7}
0.6	LOP-GS	3.4955×10^{-8}	3.4902×10^{-8}	3.4848×10^{-8}	3.4793×10^{-8}	3.4738×10^{-8}
	HKS	1.3116×10^{-6}	1.3104×10^{-6}	1.3093×10^{-6}	$1.3082 imes 10^{-6}$	1.3071×10^{-6}
0.8	LOP-GS	2.8577×10^{-8}	$2.8535 imes 10^{-8}$	2.8490×10^{-8}	2.8446×10^{-8}	2.8399×10^{-8}
	HKS	1.6133×10^{-6}	1.6122×10^{-6}	1.6111×10^{-6}	1.6100×10^{-6}	1.6089×10^{-6}
1	LOP-GS	1.0813×10^{-13}	1.0857×10^{-13}	1.0880×10^{-13}	1.0835×10^{-13}	9.8809×10^{-14}
	HKS	1.8771×10^{-6}	1.8761×10^{-6}	1.8752×10^{-6}	1.8742×10^{-6}	1.8732×10^{-6}

Table 13 Results of LOP-GS against HKS in |Error| even nodal of Situation i in Application 2 for $\mathfrak{G}_{1\zeta,n}(\xi_{\|})$

	Strategy	$\zeta_0 = 0$	$\zeta_1 = 0.25$	$\zeta_3 = 0.5$	$\zeta_3 = 0.75$	$\zeta_4=1$
0.2	LOP-GS	8.4033×10^{-5}	6.3025×10^{-5}	4.2016×10^{-5}	2.1008×10^{-5}	0
	HKS	6.7801×10^{-6}	5.0851×10^{-6}	3.3900×10^{-6}	1.6950×10^{-6}	0
0.4	LOP-GS	$1.0830 imes 10^{-4}$	8.1227×10^{-5}	5.4151×10^{-5}	2.7075×10^{-5}	0
	HKS	1.3698×10^{-5}	1.0274×10^{-5}	6.8493×10^{-6}	3.4246×10^{-6}	0
0.6	LOP-GS	9.9818×10^{-5}	7.4863×10^{-5}	4.9909×10^{-5}	2.4954×10^{-5}	0
	HKS	$2.1348 imes 10^{-5}$	1.6011×10^{-5}	$1.0674 imes 10^{-5}$	5.3370×10^{-6}	0
0.8	LOP-GS	7.5479×10^{-4}	5.6609×10^{-5}	3.7739×10^{-5}	1.8869×10^{-5}	0
	HKS	3.0556×10^{-5}	2.2917×10^{-5}	1.5278×10^{-5}	7.6391×10^{-6}	0
1	LOP-GS	$2.8948 imes 10^{-8}$	2.1711×10^{-8}	$1.4474 imes 10^{-8}$	7.2371×10^{-9}	0
	HKS	4.2419×10^{-5}	3.1814×10^{-5}	2.1209×10^{-5}	$1.0604 imes 10^{-5}$	0

 Table 14

 Results of LOP-GS against HKS in |Error| even nodal of Situation i in Application 2 for $\mathfrak{H}_{2\zeta_n n}(\xi_j)$.

	Strategy	$\zeta_0 = 0$	$\zeta_1 = 0.25$	$\zeta_3=0.5$	$\zeta_3 = 0.75$	$\zeta_4=1$
0.2	LOP-GS	8.4033×10^{-5}	6.3025×10^{-5}	4.2016×10^{-5}	2.1008×10^{-5}	0
	HKS	6.7801×10^{-6}	5.0851×10^{-6}	3.3900×10^{-6}	1.6950×10^{-6}	0
0.4	LOP-GS	1.0830×10^{-4}	8.1227×10^{-5}	5.4151×10^{-5}	2.7075×10^{-5}	0
	HKS	$1.3698 imes 10^{-5}$	$1.0274 imes 10^{-5}$	6.8493×10^{-6}	3.4246×10^{-6}	0
0.6	LOP-GS	9.9818×10^{-5}	7.4863×10^{-5}	4.9909×10^{-5}	2.4954×10^{-5}	0
	HKS	$2.1348 imes 10^{-5}$	1.6011×10^{-5}	$1.0674 imes 10^{-5}$	5.3370×10^{-6}	0
0.8	LOP-GS	7.5495×10^{-5}	5.6609×10^{-5}	3.7739×10^{-5}	1.8869×10^{-5}	0
	HKS	3.0556×10^{-5}	2.2917×10^{-5}	$1.5278 imes 10^{-5}$	7.6391×10^{-6}	0
1	LOP-GS	$2.8948 imes 10^{-8}$	2.1711×10^{-8}	$1.4474 imes 10^{-8}$	7.2372×10^{-9}	0
	HKS	$4.2419\ \times 10^{-5}$	3.1814×10^{-5}	$2.1209\ \times 10^{-5}$	1.0604×10^{-5}	0

 Table 15

 Results of LOP-GS against HKS in |Error| even nodal of Situation ii in Application 2 for $\mathfrak{H}_{1\zeta_nn}(\xi_{\tilde{j}})$.

				1 \ 1 2 /		
	Strategy	$\zeta_0 = 0$	$\zeta_1 = 0.25$	$\zeta_3 = 0.5$	$\zeta_3 = 0.75$	$\zeta_4 = 1$
0.2	LOP-GS	1.2863×10^{-5}	9.6477×10^{-6}	6.4318×10^{-6}	3.2159×10^{-6}	0
	HKS	9.3727×10^{-6}	$7.0295 imes 10^{-6}$	4.6863×10^{-6}	$2.3432 imes 10^{-6}$	0
0.4	LOP-GS	1.6043×10^{-5}	$1.2032\ imes 10^{-5}$	8.0215×10^{-6}	4.0107×10^{-6}	0
	HKS	9.9756×10^{-6}	7.4817×10^{-6}	$4.9878 imes 10^{-6}$	$2.4939 imes 10^{-6}$	0
0.6	LOP-GS	1.6810×10^{-5}	1.2608×10^{-5}	8.4054×10^{-6}	4.2027×10^{-6}	0
	HKS	1.1531×10^{-5}	8.6483×10^{-6}	5.7655×10^{-6}	2.8827×10^{-6}	0
0.8	LOP-GS	$1.3993 imes 10^{-5}$	$1.0495 imes 10^{-5}$	$6.9968 imes 10^{-6}$	3.4984×10^{-6}	0
	HKS	1.4784×10^{-5}	1.1088×10^{-5}	7.3922×10^{-6}	3.6961×10^{-6}	0
1	LOP-GS	$1.5105 imes 10^{-8}$	$1.1328 imes 10^{-8}$	7.5525×10^{-9}	3.7762×10^{-9}	0
	HKS	$2.1025 \ \times 10^{-5}$	1.5769×10^{-5}	$1.0512\ \times 10^{-5}$	5.2564×10^{-6}	0

 $\textbf{Table 16} \\ \textbf{Results of LOP-GS against HKS in } |\textbf{Error}| \ \textbf{even nodal of Situation ii in Application 2 for } \mathfrak{H}_{2\zeta_{\eta}n}\left(\xi_{\tilde{\jmath}}\right).$

	Strategy	$\zeta_0 = 0$	$\zeta_1=0.25$	$\zeta_3 = 0.5$	$\zeta_3 = 0.75$	$\zeta_4=1$
0.2	LOP-GS	1.2863×10^{-5}	9.6476×10^{-6}	6.4317×10^{-6}	3.2158×10^{-6}	0
	HKS	9.3727×10^{-6}	7.0295×10^{-6}	4.6863×10^{-6}	$2.3432 imes 10^{-6}$	0
0.4	LOP-GS	$1.6043 imes 10^{-5}$	$1.2032 imes 10^{-5}$	$8.0216 imes 10^{-6}$	$4.0108 imes 10^{-6}$	0
	HKS	9.9756×10^{-6}	7.4817×10^{-6}	$4.9878 imes 10^{-6}$	$2.4939 imes 10^{-6}$	0
0.6	LOP-GS	1.6810×10^{-5}	1.2607×10^{-5}	$8.4053 imes 10^{-6}$	4.2026×10^{-6}	0
	HKS	1.1531×10^{-5}	8.6483×10^{-6}	$5.7655 imes 10^{-6}$	2.8827×10^{-6}	0
0.8	LOP-GS	1.3994×10^{-5}	$1.0495 imes 10^{-5}$	6.9970×10^{-6}	3.4985×10^{-6}	0
	HKS	1.4784×10^{-5}	1.1088×10^{-5}	7.3922×10^{-6}	3.6961×10^{-6}	0
1	LOP-GS	1.5562×10^{-8}	1.1671×10^{-8}	7.7810×10^{-9}	3.8905×10^{-9}	0
	HKS	$2.1025 imes 10^{-5}$	1.5769×10^{-5}	$1.0512 imes 10^{-6}$	5.2564×10^{-6}	0

perior performance of the LOP-GS in certain cases can be attributed to its spectral accuracy and the global nature of the basis functions. The LOPs, being orthogonal, allow for efficient approximation of smooth solutions with fewer terms, leading to rapid convergence. In contrast, the HKS, while highly flexible and effective for scattered data or irregular domains, may involve denser system matrices and higher computational cost. Thus, for problems with smooth solutions on regular domains, the LOP-GS tends to be more accurate and computationally efficient.

Ultimately, we analyze the time complexity of the proposed LOP-GS. The implemented instructions are organized into conventional steps designed to minimize the algorithm's overall execution time. The code contains a single loop, resulting in a linear time complexity of O(N), which is considered efficient. Tables 17 and 18 present the execution times (in seconds) for the two utilized applications corresponding to the previously discussed data. Here, RT denotes the running time in seconds (LOP-GS) or minutes (HKS).

Table 17 Time complexity analysis concerning varying values of ζ_n across all situations in Application 1.

ζ-cut	Table 9		Table 10	Table 10		Table 11		Table 12	
	LOP-GS	HKS	LOP-GS	HKS	LOP-GS	HKS	LOP-GS	HKS	
ζ_{η}	RT (s)	RT (m)	RT (s)	RT (m)	RT (s)	RT (m)	RT (s)	RT (m)	
0	3.5	6	3.5	6	3	5	3	5	
0.25	3	5.5	3	5.5	2.5	4.5	2.5	4.5	
0.5	2.5	5.5	2.5	5.5	2.5	4.5	2.5	4.5	
0.75	2.5	5.5	2.5	5.5	2	4.5	2	4.5	
1	2	4.5	2	4.5	1.5	3.5	1.5	3.5	

Table 18 Time complexity analysis concerning varying values of ζ_n across all situations in Application 2.

	Table 9		Table 10		Table 11		Table 12	
ζ-cut	LOP-GS	HKS	LOP-GS	HKS	LOP-GS	HKS	LOP-GS	HKS
ζ_{η}	RT (s)	RT (m)	RT (s)	RT (m)	RT (s)	RT (m)	RT (s)	RT (m)
0	2.5	5.5	2.5	5.5	3	6	3	6
0.25	2.5	5	2.5	5	2.5	5.5	2.5	5.5
0.5	2.5	4.5	2.5	4.5	2	5.5	2	5.5
0.75	2.5	4.5	2.5	4.5	2	5.5	2	5.5
1	2	4	2	4	1.5	4	1.5	4

Therewith, time complexity is crucial in numerical analysis because it measures the efficiency of algorithms in terms of execution time as the input size grows. Efficient time complexity ensures that numerical methods remain practical and scalable for solving large-scale problems, especially in scientific computing, engineering, and data-intensive applications.

Concluding remarks

The FTDMs are an extension of CTDMs used to represent models that involve uncertainty or inaccuracy in the initial values or model parameters. These models are of great importance in many engineering and scientific applications, and their most prominent benefits are as follows:

- More realistic analysis of dynamic models: FTDMs provide powerful tools for modeling systems that contain ambiguity or noise.
- Engineering and physical applications: FTDMs are used to analyze electrical, mechanical, and hydraulic systems that contain uncertain or time-varying parameters.
- Medical and biological applications: FTDMs help in studying the spread of epidemics, physiological changes, and cell growth models, where data is often inaccurate or constantly changing.

The LOP-GS is an effective semi-analytical method for solving FTDMs, particularly for problems with moderate complexity. However, like many spectral or polynomial-based methods, it has several limitations, especially when applied to more challenging scenarios like high-dimensional systems or highly nonlinear FTDMs. Here are the main limitations:

1. Scalability to high-dimensional systems:

- Curse of dimensionality: the method's computational complexity grows rapidly with the number of dimensions, due to the need for multidimensional polynomial expansions.
- Memory and computational load: representing the solution as a sum of LOPs in multiple variables requires significant memory and can be computationally expensive.
- Basis function explosion: in higher dimensions, the number of basis functions increases combinatorially, making the Galerkin system very large and harder to solve.

2. Handling highly nonlinear fuzzy systems:

- Nonlinearity treatment: GS, especially with orthogonal polynomials like Lucas, can struggle with strongly nonlinear terms due to difficulty in projecting nonlinear terms onto the basis space and possible loss of orthogonality or approximation accuracy.
- Fuzzy arithmetic complexity: nonlinear fuzzy operations introduce additional complexity, especially when using ζ-cut formation or Hukuhara derivatives.
- Error accumulation: in nonlinear systems, approximation errors from truncation or projection may amplify over time or space, leading to reduced reliability.

Anyhow, this article presents an innovative LOP-GS that utilizes LOPs as basis functions in the weighted residual GS to approximate the fuzzy solutions of FTDMs. These models are first transformed into two corresponding situations as CTDM forms. For each situation, the required functions are expressed in terms of LOPs, and the residual function is computed to formulate a set of transcendental equations. By solving the resulting set, numerical approximations are obtained. The LOP-GS is applied under the constraints of SGD to efficiently produce fuzzy approximations for specific FTDMs. The approach is particularly advantageous due to its high accuracy, especially in nonhomogeneous cases, even with a small number of iterations. The gained results support the convergence, demonstrating that the approximation error shrinks monotonically as the measure of terms increases. Furthermore, we discuss error estimation in LOP-GS with comparisons with the HKS. In a future study, we may explore the approximation of conformable FTDMs using the LOP-GS.

CRediT authorship contribution statement

Omar Abu Arqub: Writing – original draft, Validation, Resources, Project administration, Funding acquisition, Formal analysis. Marwan Abukhaled: Writing – review & editing, Writing – original draft, Visualization, Validation, Supervision, Software. Hind Sweis: Writing – original draft, Validation, Software, Methodology, Investigation, Data curation, Conceptualization. Nabil Shawagfeh: Supervision, Resources, Project administration, Investigation.

Declaration of competing interest

The authors declare that they have no known competing financial interests or personal relationships that could have appeared to influence the work reported in this paper.

Declarations

Conflicts of Interest: The authors declare that they have no conflicts of interest.

Data Availability Statement: No datasets are associated with this manuscript. The datasets used for generating the plots and results during the current study can be directly obtained from the numerical simulation of the related mathematical equations in the manuscript.

Consent to Participate and Publish: The authors declare that they participated in this paper willingly, and the authors declare consent to the publication of this paper.

Funding Statement: The authors declare that no funds, grants, or other support were received during the preparation of this manuscript.

Ethical Approval: This article does not contain any studies with human participants or animals performed by any of the authors.

Acknowledgment

The work in this study was supported, in part, by the Open Access Program from the American University of Sharjah. This study represents the opinions of the author(s) and does not mean to represent the position or opinions of the American University of Sharjah.

Data availability

No data was used for the research described in the article.

References

- S. Yu, Z. Xu, Generalized Intuitionistic Multiplicative Fuzzy Calculus Theory and Applications, Springer, Germany, 2020.
- [2] L.T. Gomes, L.C. de Barros, B. Bede, Fuzzy Differential Equations in Various Approaches, Springer, Germany, 2015.
- [3] Y.K. Kyosev, K.G. Peeva, Fuzzy Relational Calculus: Theory, Applications and Software, World Scientific Publishing Company, Singapore, 2005.
- [4] S. Song, C. Wu, Existence and uniqueness of solutions to the Cauchy problem of fuzzy differential equations, Fuzzy. Sets. Syst. 110 (2000) 55–67.
- [5] J.J. Buckley, T. Feuring, Fuzzy differential equations, Fuzzy. Sets. Syst. 110 (2000)
- [6] E. Hüllermeier, An approach to modelling and simulation of uncertain systems, Int. J. Uncertain. Fuzziness Knowl.-Based Syst. 5 (1997) 117–137.
- [7] X.M. Liu, J. Jiang, L. Hong, A numerical method to solve a fuzzy differential equation via differential inclusions, Fuzzy. Sets. Syst. 404 (2021) 38–61.
- [8] M.T. Mizukoshi, L.C. Barros, Y. Chalco-Cano, H. Román-Flores, R.C. Bassanezi, Fuzzy differential equations and the extension principle, Inf Sci (Ny) 177 (2007) 3627–3635.
- [9] M.M. Diniz, L.T. Gomes, R.C. Bassanezi, Optimization of fuzzy-valued functions using Zadeh's extension principle, Fuzzy. Sets. Syst. 404 (2021) 23–37.
- [10] B. Bede, S.G. Gal, Almost periodic fuzzy-number-valued functions, Fuzzy. Sets. Syst. 147 (2004) 385–403.
- [11] B. Maayah, O. Abu Arqub, uncertain M-fractional differential problems: existence, uniqueness, and approximations using Hilbert reproducing technique provisioner with the case application: series resistor-inductor circuit, Phys. Scr. 99 (2024) 025220.
- [12] O. Abu Arqub, R. Mezghiche, B. Maayah, Fuzzy M-fractional integrodifferential models: theoretical existence and uniqueness results, and approximate solutions utilizing the Hilbert reproducing kernel algorithm, Front. Phys. 11 (2023) 1252919.

- [13] O. Abu Arqub, J. Singh, B. Maayah, M. Alhodaly, Reproducing kernel approach for numerical solutions of fuzzy fractional initial value problems under the Mittag-Leffler kernel differential operator, Math. Methods Appl. Sci. 46 (2023) 7065-7096
- [14] O. Abu Arqub, J. Singh, M. Alhodaly, Adaptation of kernel functions-based approach with Atangana–Baleanu–Caputo distributed order derivative for solutions of fuzzy fractional Volterra and Fredholm integrodifferential equations, Math. Methods Appl. Sci. 6 (2023) 7807–7834.
- [15] S.A.M. Jameel, S. Karim, A.F. Jameel, Applying the least squares approach to solve Fredholm fuzzy fractional integro-differential equations, J. Appl. Sci. Eng. 28 (2024) 2005–2015.
- [16] P. Filipponi, A.F. Horadam, Second derivative sequences of Fibonacci and Lucas polynomials, Fibonacci Q. 31 (1993) 194–204.
- [17] J. Wang, On the kth derivative sequences of Fibonacci and Lucas polynomials, Fibonacci Q. 33 (1995) 174–178.
- [18] Z. Akyuz, S. Halici, On some combinatorial identities involving the terms of generalized Fibonacci and Lucas sequences, Hacet. J. Math. Stat. 42 (2013) 431–435.
- [19] E. Özkan, I. Altun, Generalized Lucas polynomials and relationships between the Fibonacci polynomials and Lucas polynomials, Commun. Algebra 47 (2019) 4020–4030
- [20] W.M. Abd-Elhameed, A. Napoli, Some novel formulas of Lucas polynomials via different approaches, Symmetry. (Basel) 15 (2013).
- [21] S. Haq, I. Ali, Approximate solution of two-dimensional Sobolev equation using a mixed Lucas and Fibonacci polynomials, Eng. Comput. 38 (2022) 2059–2068.
- [22] Ö. Oruç, A new numerical treatment based on Lucas polynomials for 1D and 2D sinh-gordon equation, Commun. Nonlinear. Sci. Numer. Simul. 57 (2018) 14–25.
- [23] M.N. Sahlan, H. Afshari, Lucas polynomials based spectral methods for solving the fractional order electrohydrodynamics flow model, Commun. Nonlinear. Sci. Numer. Simul. 107 (2022) 106108.
- [24] I. Area, E. Godoy, A. Ronveaux, A. Zarzo, Solving connection and linearization problems within the Askey scheme and its q-analogue via inversion formulas, J. Comput. Appl. Math. 133 (2001) 151–162.
- [25] Ö. Oruç, A new algorithm based on Lucas polynomials for approximate solution of 1D and 2D nonlinear generalized Benjamin–Bona–Mahony–Burgers equation, Comput. Math. Appl. 74 (2017) 3042–3057.
- [26] Y.H. Youssri, S.M. Sayed, A.S. Mohamed, E.M. Aboeldahab, W.M. Abd-Elhameed, Modified Lucas polynomials for the numerical treatment of second-order boundary value problems, Comput. Methods Differ. Equ. 11 (2023) 12–31.
- [27] W.M. Abd-Elhameed, Y.H. Youssri, Spectral Solutions for fractional differential equations via a novel Lucas operational matrix of fractional derivatives, Rom. J. Phys. 61 (2016) 795–813.
- [28] M.A. El-Hady, Mohamed El-Gamel, M. Izadi, A. El-Shenawy, Numerical computation of nonlinear boundary value problems in heat transfer and chemical engineering: a robust Lucas–Fibonacci series approach, J. Taibah Univ. Sci. 9 (2025) 2477917.
- [29] M.A. Yousif, F.K. Hamasalh, Conformable non-polynomial spline method: a robust and accurate numerical technique, Ain Shams Eng. J. 15 (2024) 102415.
- [30] M.A. Yousif, R.P. Agarwal, P.O. Mohammed, A.A. Lupas, R. Jan, N. Chorfi, Advanced methods for conformable time-fractional differential equations: logarithmic non-polynomial splines, Axioms 13 (2024) 551.
- [31] R. Goetschel, W. Voxman, Elementary fuzzy calculus, Fuzzy. Sets. Syst. 18 (1986) 31–43.
- [32] M.L. Puri, Fuzzy random variables, J. Math. Anal. Appl. 114 (1986) 409–422.
- [33] B. Bede, S.G. Gal, Generalizations of the differentiability of fuzzy number value functions with applications to fuzzy differential equations, Fuzzy. Sets. Syst. 151 (2005) 581–599.
- [34] M.L. Puri, D.A. Ralescu, Differentials of fuzzy functions, J. Math. Anal. Appl. 91 (1983) 552–558.
- [35] Y. Chalco-Cano, H. Román-Flores, On new solutions of fuzzy differential equations, Chaos Solit. Fractals 38 (2008) 112–119.
- [36] O. Kaleva, A note on fuzzy differential equations, Nonlinear analysis: theory, Methods Appl. 64 (2006) 895–900.
- [37] J.J. Nieto, A. Khastan, K. Ivaz, Numerical solution of fuzzy differential equations under generalized differentiability, Nonlinear Anal.: Hybrid Syst. 3 (2009) 700–707.